

1 **The impact of across-slope forest strips on**
2 **hillslope subsurface hydrological dynamics**

3 Leo M. Peskett^{a,b*}

4 Alan M. MacDonald^b

5 Kate V. Heal^a

6 Jeffrey J. McDonnell^{c,d}

7 Jon E. Chambers^e

8 Sebastian Uhlemann^{e,1}

9 Kirsty A. Upton^b

10 Andrew Z. Black^f

11

12 ^aUniversity of Edinburgh, School of GeoSciences, Crew Building, Alexander
13 Crum Brown Road, Edinburgh EH9 3FF, United Kingdom leo.peskett@ed.ac.uk

14 ^bBritish Geological Survey, The Lyell Centre, Research Avenue South,
15 Edinburgh EH14 4AP, United Kingdom

16 ^cGlobal Institute for Water Security, School of Environment and Sustainability,
17 University of Saskatchewan, Saskatoon SK S7N 3H5, Canada

18 ^dSchool of Geography, Earth and Environmental Sciences, University of
19 Birmingham, Birmingham B15 2TT, United Kingdom

20 ^eBritish Geological Survey, Environmental Science Centre, Nicker Hill,
21 Keyworth, Nottingham NG12 5GG, United Kingdom

22 ^fGeography and Environmental Science, Tower Building, University of Dundee,
23 Dundee DD1 4HN, United Kingdom

24 ***Corresponding author:** Leo Peskett, leo.peskett@ed.ac.uk

1 ¹ Present address: Earth & Environmental Sciences, Lawrence Berkeley National
2 Laboratory, Berkeley, CA 94720, USA

25

26 **Highlights**

- 27 • Soil moisture, groundwater and ERT data reveal moisture dynamics of a
28 forest strip
- 29 • Sub-surface moisture dynamics altered within strip but not beyond 15
30 m downslope
- 31 • Water table depths within the forest are lower than the surrounding
32 grassland
- 33 • Forest strip had no impact on groundwater connectivity during larger
34 storms

35

36 **Keywords**

37 Electrical resistivity tomography (ERT); flooding; forest strip; groundwater;
38 runoff; soil moisture

39

40 **Abstract**

41 Forest cover has a significant effect on hillslope hydrological processes
42 through its influence on the water balance and flow paths. However,
43 knowledge of how spatial patterns of forest plots control hillslope hydrological
44 dynamics is still poor. The aim of this study was to examine the impact of an
45 across-slope forest strip on sub-surface soil moisture and groundwater
46 dynamics, to give insights into how the structure and orientation of forest
47 cover influences hillslope hydrology. Soil moisture and groundwater dynamics
48 were compared on two transects spanning the same elevation on a 9°
49 hillslope in a temperate UK upland catchment. One transect was located on

50 improved grassland; the other was also on improved grassland but included a
51 14 m wide strip of 27-year-old mixed forest. Sub-surface moisture dynamics
52 were investigated upslope, underneath and downslope of the forest over 2
53 years at seasonal and storm event timescales. Continuous data from point-
54 based soil moisture sensors and piezometers installed at 0.15, 0.6 and 2.5 m
55 depth were combined with seasonal (~ bi-monthly) time-lapse electrical
56 resistivity tomography (ERT) surveys. Significant differences were identified in
57 sub-surface moisture dynamics underneath the forest strip over seasonal
58 timescales: drying of the forest soils was greater, and extended deeper and
59 for longer into the autumn compared to the adjacent grassland soils. Water
60 table levels were also persistently lower in the forest and the forest soils
61 responded less frequently to rainfall events. Downslope of the forest, soil
62 moisture dynamics were similar to those in other grassland areas and no
63 significant differences were observed beyond 15 m downslope, suggesting
64 minimal impact of the forest at shallow depths downslope. Groundwater levels
65 were lower downslope of the forest compared to other grassland areas, but
66 during the wettest conditions there was evidence of upslope-downslope water
67 table connectivity beneath the forest. The results indicate that forest strips in
68 this environment provide only limited additional sub-surface storage of rainfall
69 inputs in flood events after dry conditions in this temperate catchment
70 setting.

71 **1 Introduction**

72 There is renewed interest in forest strips (often termed “field boundary
73 planting”, “shelterbelts” or “buffer strips”) as a flood management tool in wet
74 upland environments (Dadson et al., 2017; Lane, 2017; Soulsby et al., 2017).
75 Past work in the UK has shown that forest shelterbelts in improved grassland
76 can control surface runoff (Wheater et al., 2008; Wheater and Evans, 2009).
77 This work, and other studies, have reported significant increases in soil water
78 storage capacity in shallow soils and increased infiltration rates within forest
79 strips, and evidence of forest rain shadow effects on soil moisture in adjacent
80 grassland (Jackson et al., 2008; Lunka and Patil, 2016; Marshall et al., 2009).
81 Thus understanding the impacts of forest strips on subsurface hydrology
82 appears key for controlling surface runoff and such interventions have the
83 potential for “reducing run-off even when only present as a small proportion
84 of the land cover” (Carroll et al., 2004, p. 357). If these findings can be
85 generalised, there are obvious applications within a catchment management
86 perspective for reducing flood risk. They are also important globally, given
87 rapid changes in land use towards more mosaic landscapes and the effects
88 this might have on hydrological processes (Haddad et al., 2015; Ziegler et al.,
89 2004; Zimmermann et al., 2006).

90

91 While some evidence of forest strip impacts on hillslope hydrology exists,
92 there has been limited mechanistic investigation of forest strip impacts on
93 hillslope runoff processes. Of course, mechanistic studies on single completely
94 forested hillslopes have been conducted for decades (Hewlett and Hibbert,
95 1967; Tromp-van Meerveld and McDonnell, 2006; Wenninger et al., 2004). But
96 the ‘black box’ before and after treatments applied at the catchment scale
97 (e.g. Hornbeck et al., 1970; Swank et al., 1988) have not been conducted at

98 the hillslope scale. At best there are some hillslope intercomparisons
99 (Bachmair and Weiler, 2012; Scherrer et al., 2007; Uchida et al., 2006, 2005)
100 that explore hillslope response under different land covers. All of these
101 approaches suffer from difficulties in controlling for significant heterogeneities
102 even at the plot scale, a reliance on point-based data, and the challenges that
103 these raise for developing transferable process understanding (Bachmair and
104 Weiler, 2012).

105

106 Therefore, whilst plot scale studies have shown measurable impacts of forest
107 cover on local hydrology, the use and application of these findings to assess
108 the effectiveness of forest strip planting at the hillslope scale is limited.

109 Specifically, forest strip planting raises important additional questions related
110 to the location and structure of forest cover in landscapes and its interaction
111 with other physical hillslope properties. For example, forest strips or
112 vegetation patches in more arid environments appear to 'interrupt' hydraulic
113 connectivity across landscapes (Fu et al., 2009; Liu et al., 2018) so may have
114 variable effects on downslope hydrological processes. However, such
115 questions have only been looked at in a few modelling studies (Reaney et al.,
116 2014).

117

118 Here we examine the influence of a forest strip on hillslope sub-surface
119 hydrological dynamics. We focus on a typical example of a narrow (14 m
120 wide), mixed forest shelterbelt planted on improved grassland (land used for
121 grazing that has been improved through management practices such as
122 liming or drainage) - a configuration similar to that being used in some
123 'natural' flood risk management schemes in the UK (Environment Agency,
124 2018; Tweed Forum, 2019). We pair hillslope scale soil moisture and

125 groundwater level measurements with time-lapse electrical resistivity
126 tomography (ERT) to help extrapolate from point-based measurements to
127 hillslope scale process understanding. We build on work by Cassiani et al.
128 (2012), Garcia-Montiel et al. (2008) and Jayawickreme et al. (2008), extending
129 the ERT technique to investigate the interaction of two vegetation types and
130 spatial orientation on the slope. Our specific questions are:

- 131 1. How do across-slope forest strips alter soil moisture and groundwater level
132 dynamics beneath the forest?
- 133 2. Do forest strips have downslope impacts on soil moisture and groundwater
134 level dynamics?

135

136 We consider these questions over seasonal and storm event timescales, and
137 also the potential implications from a flood risk management perspective.

138

139 **2 Methods**

140 **2.1 Site description**

141 The experiment was established on a hillslope in the 67 km² Eddleston Water
142 catchment, a tributary of the River Tweed in the Scottish Borders, UK (Figure
143 1). The catchment hosts an ongoing project initiated in 2010 to investigate
144 the impact of natural flood management (NFM) measures aimed at controlling
145 runoff from farmland and forest land (Werritty et al., 2010). The measures
146 include tree-planting, establishment of holding ponds on farmland, re-
147 meandering the Eddleston Water river, and the construction of 'leaky' dams in
148 some sub-catchments (Tweed Forum, 2019).

149

150 Catchment characteristics are typical of much of the UK uplands. Topography
151 is varied with elevations of 180-600 m and the climate is cool with mean

152 annual precipitation of 1180 mm (at Eddleston village, 2011-2017), falling
153 mainly as rainfall. Mean daily temperatures range from 3 °C in winter to 13
154 °C. Daily evapotranspiration ranges from 0.2 mm in winter to 2.5 mm in
155 summer (estimated using the Granger-Gray method (Granger and Gray, 1989)
156 using data from the weather station in the catchment at Eddleston village).
157 Bedrock throughout most of the catchment is comprised of Silurian
158 impermeable well-cemented, poorly sorted sandstone greywackes (Auton,
159 2011). Extensive glaciation has affected the superficial geology and soil
160 types. Soils on steeper hillsides are typically freely draining brown soils
161 overlying silty glacial till, rock head or weathered head deposits. Towards the
162 base of the hillslopes the ground is typically wetter and soils comprise
163 sequences of gleyed clays and peats on sub-angular head deposits or alluvial
164 deposits closer to the river. Land cover is mainly improved or semi-improved
165 grassland on the lower slopes and rough heathland at higher elevations.
166 Forest cover is typically mixed coniferous and deciduous woodland,
167 concentrated along field boundaries.

168

169 The experimental hillslope is located ~100-200 m from the Eddleston Water
170 rising to 30 m above the river with a relatively uniform slope of ~9°. Soil pit
171 surveys (0.7 m depth) found that soils comprise typically 0.15-0.20 m deep
172 silty cambisols containing numerous sub-angular cobbles up to 60 mm length.
173 Large roots (< 30 mm) were prevalent in the top 0.20 m of the forest soils,
174 with occasional large tree roots and frequent smaller tree roots (<5 mm)
175 present down to the bottom of the soil pits. By contrast, small roots were
176 prevalent in the top 0.20 m of the grassland soils, with no roots identified at
177 the base of the soil pits (Figure S1). Borehole logs (Figure S1) and a grid of
178 initial ERT surveys showed a clear layered structure to the underlying

179 geology, with soils above a layer of silt/loam glacial till containing numerous
180 large cobbles, which transition at 1.5-2 m depth into sub-angular head
181 deposits or weathered rock head.

182

183 Soils on the hillslope are generally freely draining, although surface runoff
184 was observed at the wettest times of year in the area upslope of the forest
185 strip. Hydraulic conductivity of soils overlying head deposits has been
186 measured as part of the wider project on a similar hillslope 2 km to the north
187 which found median values of 21-39 mm h⁻¹ (0.50-0.94 m d⁻¹) for improved
188 grassland and 42 mm h⁻¹ (1 m d⁻¹) for an ~50 year old plantation forest, and
189 119-174 mm h⁻¹ (2.86-4.18 m d⁻¹) for broadleaf forests > 180 years old
190 (Archer et al., 2013). The hydraulic conductivity of the glacial till was
191 estimated to range from <0.001 to 1 m d⁻¹ based on data from other locations
192 in Scotland (MacDonald et al., 2012). Hydraulic conductivities of the
193 underlying head deposits could not be measured directly using falling head
194 tests in the piezometers as values were beyond the design limit of the test
195 methodology (40 m d⁻¹). However, elsewhere in the Eddleston catchment, the
196 permeability of the head deposits has been measured as 500 m d⁻¹ (Ó
197 Dochartaigh et al., 2018). Hydraulic conductivity of the bedrock was not
198 measured, but Silurian greywacke aquifers elsewhere in southern Scotland
199 have been shown to have low productivity (Ó Dochartaigh et al., 2015), with
200 an estimated average transmissivity of 20 m² d⁻¹ (Graham et al., 2009).

201

202 Particle size and organic matter content were determined from soil samples
203 taken at 0.15 m and 0.6 m depth at all 14 soil moisture monitoring sites
204 (Table S1). Particle size analysis used the sieving method for the proportion
205 above 2 mm and a Beckmann Coulter LS230 particle size analyser for the

206 proportion below 2 mm, according to international standards (ASTM
207 International, 2004). The soil texture is predominately silty loam with a
208 substantial proportion of gravel and cobbles (22-58% by mass). There is little
209 variation between locations and transects, although the 0.6 m depth sample
210 at the top of the grassland transect and one of the 0.15 m depth samples in
211 the forest strip had slightly higher sand content than the other locations.
212 Organic content was measured for the same samples using the loss on
213 ignition method at 375 °C for 24 hours (Ball, 1964), and was 2-7%.

214

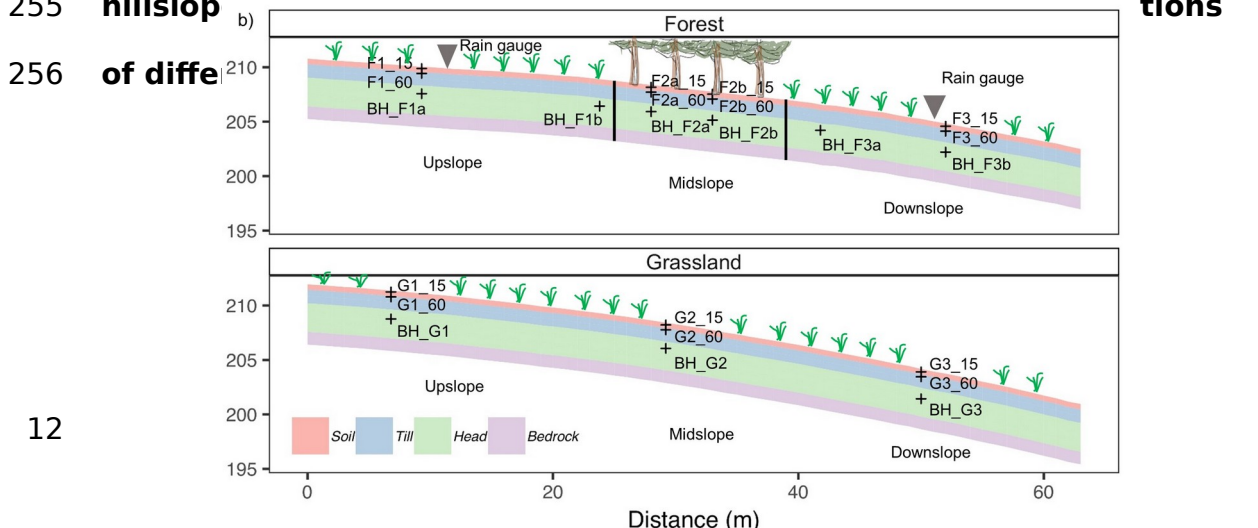
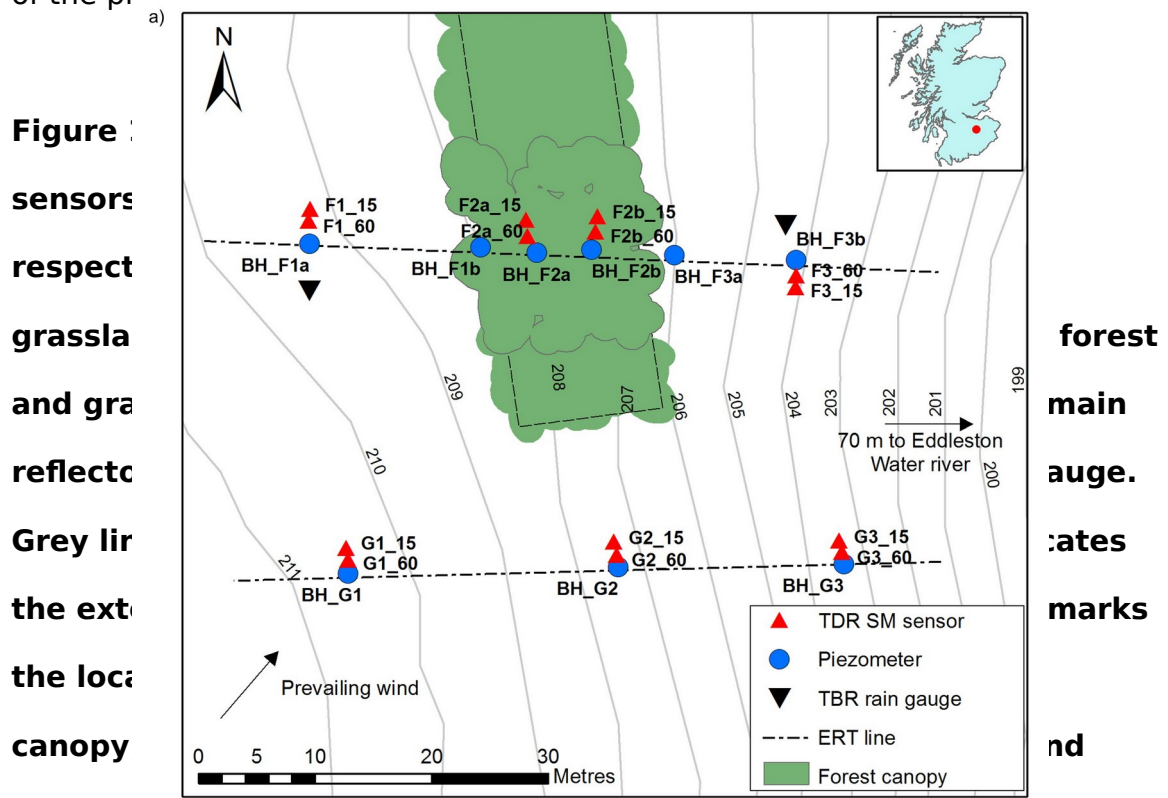
215 **2.2 Experimental setup**

216 The experiment consisted of two 64 m instrumented transects established at
217 the same topographic elevation (212-195 m) on the hillslope and separated
218 by 30 m (Figure 1). One transect was on improved grassland, whilst the other
219 intersected, and was centred on, a 14 m wide strip of 27 year old fenced
220 mixed forest containing Sitka spruce (*Picea sitchensis*), European larch (*Larix*
221 *decidua*), ash (*Fraxinus excelsior*), hawthorn (*Crataegus monogyna*), oak
222 (*Quercus robur*) and elder (*Sambucus nigra*). Tree height ranged from 7 to 14
223 m and rooting depths were estimated as 0-1.5 m for Sitka spruce and 0-2.5 m
224 for the deciduous trees, based on trees of similar age on similar soils (Crow,
225 2005; Fraser and Gardiner, 1967). Both land cover types are typical of the
226 wider catchment and much of the UK uplands, with the grassland used
227 throughout the year for grazing sheep and occasionally horses.

228

229 Fourteen soil moisture sensors (Delta-T SMT150 with GP4 loggers) were
230 installed in pairs at 0.15 m and 0.6 m depth at upslope, midslope and
231 downslope elevations in each transect (3 pairs on the grassland and 4 pairs
232 on the forest transect). Nine 50 mm-diameter piezometers were installed at

233 2.5 m depth using a hand held rock drill at similar locations to the soil
 234 moisture sensors (3 on the grassland and 6 on the forest transect). The
 235 additional piezometers on the forest transect were installed close to the
 236 upslope and downslope boundaries of the forest. All piezometers were sealed
 237 with bentonite to 0.6 m depth and contained a 0.35 m screen at their base. All
 238 piezometers were instrumented with non-vented Rugged TROLL 100 loggers
 239 logging at 15-minute intervals and levels were checked manually every 3
 240 months. A barometric logger (Rugged BaroTROLL 100) at the site was used to
 241 correct for atmospheric pressure. Two tipping bucket rain gauges were
 242 installed 16 m upslope and downslope of the forest to check for the influence
 243 of the prevailing wind on rainfall on either side of the forest (Figure 1)



257 The logging period was November 2016 to November 2018 inclusive. One of
258 the soil moisture and rainfall loggers failed on the forest transect, resulting in
259 a ~5-month data gap for the shallow soil moisture sensor at the top of the
260 transect (F1_15), a ~3-month gap in the upslope rain gauge, and a ~1-month
261 gap in data for the other three sensors attached to this logger. The
262 groundwater data was also discontinuous due to large seasonal variations in
263 groundwater level leading to water table levels below the level of the sensors.
264 The gaps in data have been taken into account in the analysis where
265 necessary. Additionally, one of the upper soil moisture sensors in the forest
266 (F2b_15) did not respond for any event, perhaps because it was in an air
267 pocket, and was removed from the analysis. Two piezometers (BH_F2b,
268 BH_F3b) which did not respond during the study period were also removed
269 from the analysis.

270

271 Two soil temperature probes (Delta-T ST4) were installed at 0.15 m and 0.6 m
272 depth at the top of the grassland transect, and temperature data were also
273 collected from the pressure transducers at 2.5 m depth. Air temperature, wind
274 speed and direction, solar radiation and rainfall data were obtained from an
275 automated weather station 3 km north of the site at Eddleston village and a
276 similar elevation of 200 masl. These datasets were used to estimate
277 evapotranspiration and to infill missing rainfall data as explained in section
278 2.3.2. Most of the trees closest to the transect in the forest are conifers, but
279 the deciduous trees had no leaves between mid-November and mid-April.

280

281 Initial 2D ERT surveys consisting of 6 lines at 2 m spacing were carried out in
282 August 2016 across and down the slope to help characterise the geological
283 structure of the site. A series of ten repeated 2D ERT surveys were then

284 conducted between November 2016 and April 2018 along the forest and
285 grassland transects. The surveys were undertaken using an AGI SuperSting
286 R8 imaging system connected to arrays of 64 stainless steel pin electrodes
287 positioned at 1 m intervals. Measurements were made using the dipole-dipole
288 configuration with dipole sizes (a), of 1, 2, 3 and 4 m and unit dipole
289 separations (n) of 1-8a. Time-lapse inversion of the data was performed using
290 RES2DINV (Loke et al., 2013), which employs a regularised least-squares
291 optimisation approach, in which the forward problem was solved using the
292 finite-element method.

293

294 **2.3 Soil moisture and groundwater data analysis**

295 The soil moisture and groundwater data were analysed using the whole time
296 series to understand annual changes and through the selection of specific
297 events to understand event dynamics. The whole time series data and event
298 data were also examined on a seasonal basis, with the following definitions:
299 Winter ('Wi': Dec-Feb), Spring ('Sp': Mar-May), Summer ('Su': Jun-Aug) and
300 Autumn ('Au': Sep-Nov), These periods were defined based on the soil
301 moisture data that showed full wetting up did not occur until late Nov-early
302 Dec, providing a better baseline for comparison.

303

304 **2.3.1 Whole time series analysis**

305 Soil moisture and groundwater level data were first analysed for the whole
306 time series to give an indication of seasonal patterns, discontinuities in the
307 groundwater data and logger errors. Summary statistics included median
308 values; minimum and maximum values; interquartile range; and graphical
309 inspection of wetting up and recession characteristics. Given the discontinuity
310 of the groundwater data, only the proportion of the year for which a water

311 table was recorded and the range in levels were of interest, along with more
312 descriptive details (e.g. recession behaviour) of the water table response to
313 rainfall events.

314

315 **2.3.2 Event analysis**

316 Soil moisture and groundwater events were selected for analysis by first
317 identifying rainfall events and then finding the associated event in the soil
318 moisture/groundwater time series. The rainfall events were selected
319 automatically from the upslope rain gauge time series based on a total event
320 rainfall of ≥ 8 mm and an intensity criterion that an event contained no period
321 longer than 2 hours without rainfall. This resulted in 56 events, which was
322 reduced to 52 events as described in the following paragraph. Characteristics
323 were calculated for each event in the final event dataset, including total
324 rainfall (TR, ranging from 8.2 to 52.6 mm), mean hourly intensity (I, ranging
325 from 0.5 to 2.5 mm h⁻¹), a 5-day weighted antecedent wetness index (AWI,
326 ranging from 1.3 to 48.3 mm) (Kohler and Linsley, 1951) and the 28-day
327 antecedent rainfall (AP28d, ranging from 13.2 to 138 mm). The gap in the
328 upslope rainfall gauge time series from 01/09/2017 - 02/12/2017 was filled
329 directly with data from the weather station at Eddleston village, which was
330 considered appropriate based on the small differences in rainfall recorded
331 across multiple sites in the catchment. A full summary of the selected events
332 is given in Table S2.

333

334 Events in the time series for the operational 13 soil moisture sensors were
335 initially selected automatically by locating the point after the start of event
336 rainfall where the 1-hour rolling mean smoothed soil moisture exceeded a
337 gradient threshold of >0.001 m³ m⁻³ h⁻¹ and where the total change in soil

338 moisture was $>0.012 \text{ m}^3 \text{ m}^{-3} \text{ h}^{-1}$. Events in the time series for the seven
339 operational groundwater sensors were selected in the same way but with a
340 gradient threshold of $>0.008 \text{ m h}^{-1}$ and where the total change in
341 groundwater level was $>0.001 \text{ m h}^{-1}$ in the 1-hour smoothed groundwater
342 data. These thresholds were determined iteratively by graphical inspection of
343 several randomly selected events from each sensor. Saturation behaviour was
344 identified in some of the soil moisture time series as a rapid rise in soil
345 moisture to near saturation, followed by a plateauing in soil moisture and
346 then a rapid decrease in value, which was captured in the algorithm using a
347 combination of the gradient of the rising limb and the maintenance of a peak
348 within 95% of the peak level for more than 1.5 h.

349

350 Given the variety in types of response, all selected events were inspected
351 manually. Four events were removed completely due to excessive noise, even
352 in the smoothed soil water and groundwater time series, leading to spurious
353 event characteristics across all locations. Further manual adjustments were
354 made for particular locations in some events to adjust start and peak
355 selection due to excessive noise and to correct peaks where very close
356 consecutive events resulted in peak selection associated with the subsequent
357 event. The final event dataset consisted of 52 events (Table S2).

358

359 The following metrics were calculated for each event, including: whether
360 response occurred in the soil moisture or groundwater data (R); time to
361 response from the start of rainfall (TTR); time to peak from start of rainfall
362 (TTPR); and maximum absolute rise (MR). Response was defined by the
363 criteria above including, in the case of the piezometers, those that rose from
364 an initially dry state.

365

366 Comparison of R, TTR, TTPR and MR between grassland and forest transects
367 was made for a subset of nine events at the wettest points in the time series
368 when the piezometer downslope of the forest responded (and most other
369 sensors were also responding), to enable comparison of sensors with a more
370 balanced design. Pairwise comparisons between sensors in the same domains
371 (upslope, midslope and downslope) and depths on the different transects
372 were also made for all responding sensors in the pair to enable analysis under
373 a wider range of conditions. Tests for normality (Shapiro-Wilk) and
374 homoscedasticity (Fligner-Killeen) were conducted prior to statistical testing.
375 These showed that with a \log_{10} transformation the majority of sensor datasets
376 followed a normal distribution and all of them were homoscedastic. Given
377 some deviation from normality but relatively uniform differences in variance,
378 the non-parametric Kruskal-Wallis test was used to compare medians and
379 Dunn's post-hoc test to determine where any significant differences occurred.

380

381 Logistic regression was used to test the relationship between event
382 characteristics and whether sensors responded given the binary nature of the
383 data. Spearman's rank correlation was used to assess associations between
384 event characteristics and TTR, TTPR and MR. Prior to the exploration of the
385 relationship between event characteristics and response metrics, co-linearity
386 between the different event characteristics was checked (Table S3). There
387 was some co-linearity between event rainfall and event intensity, and also
388 AWI and AP28d, which was considered in the interpretation of the results. All
389 statistical analyses were conducted in R version 3.5.1 with significance
390 defined as $p < 0.05$.

391

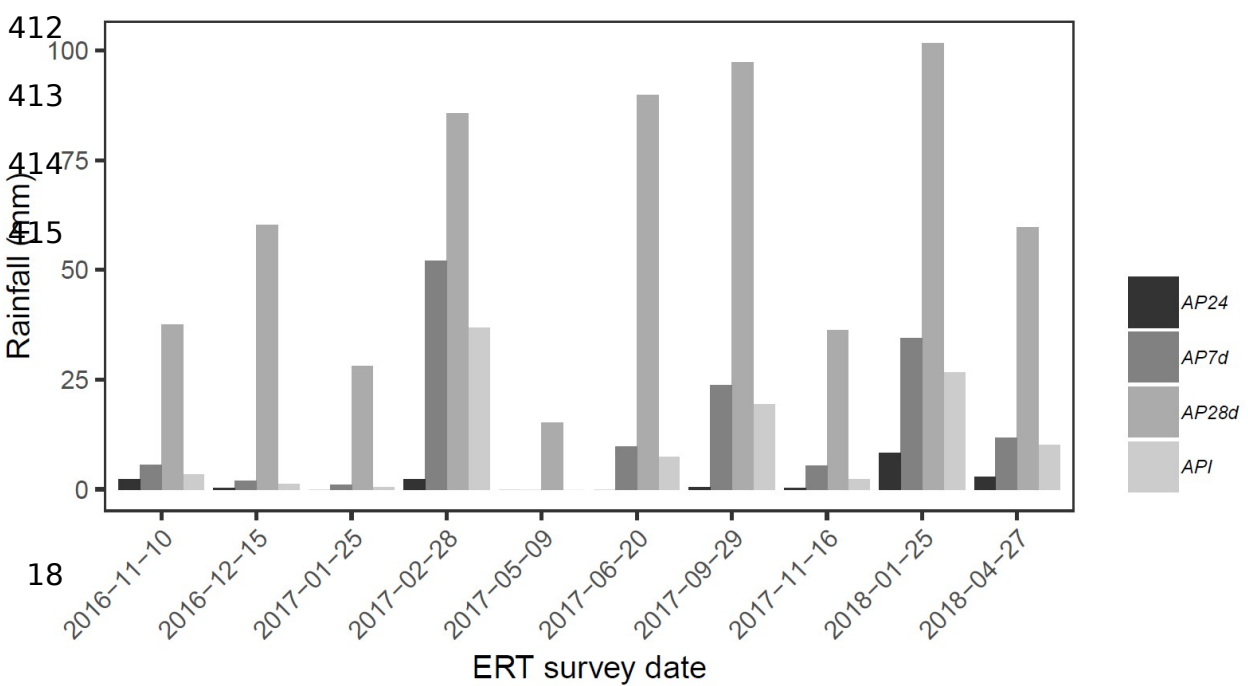
392 **2.4 ERT data analysis**

393 The ERT surveys were carried out following variable antecedent rainfall
394 conditions (Figure 2). After correction of the ERT model for effects of soil
395 temperature using data from the nested temperature probes (at 0.15 m and
396 0.6 m depth) and the BH_G1 pressure transducer at 2.5 m depth, temporal
397 changes in resistivity between the surveys were assumed to be due to
398 changes in soil moisture content, based on relationships established in other
399 studies (Brunet et al., 2010; Cassiani et al., 2009; Chambers et al., 2014). To
400 factor out potential differences between material properties, comparisons in
401 each of the transects were made relative to the May 2017 survey as it was
402 the driest survey with the highest resistivities.

403

404 Resistivity contrasts between depths and locations on the different transects
405 were analysed by averaging resistivities across different lateral or vertical
406 groups of cells in the ERT datasets from each of the transects. Given some
407 deviation from normality in resistivity distributions within groups, median
408 resistivities were compared using the same non-parametric tests as for the in-
409 situ sensor data and a bias-corrected bootstrapping procedure used to
410 estimate confidence intervals for each group.

411



416 **3 Results**

417 **3.1 Seasonal sub-surface hydrological dynamics**

418 **3.1.1 Soil moisture content and groundwater level**

419 Soil moisture content had a distinct seasonal pattern, with generally drier
420 conditions in summer and wetter in winter. This was most pronounced in the
421 shallow soil moisture sensors and lasted longer in the forest compared to the
422 grassland (April to December and April to July, respectively) (Figure 3).

423 Saturation occurred during winter in most of the soil moisture time series on
424 grassland areas as distinct plateaued peaks that also recessed rapidly (Figure
425 3). In most instances this was due to infiltration, but occasionally at locations
426 F1_60 and G2_60 the water table rose above the level of the soil moisture
427 sensor. Saturated soil moisture conditions were not apparent in the forested
428 areas (F2 sensors).

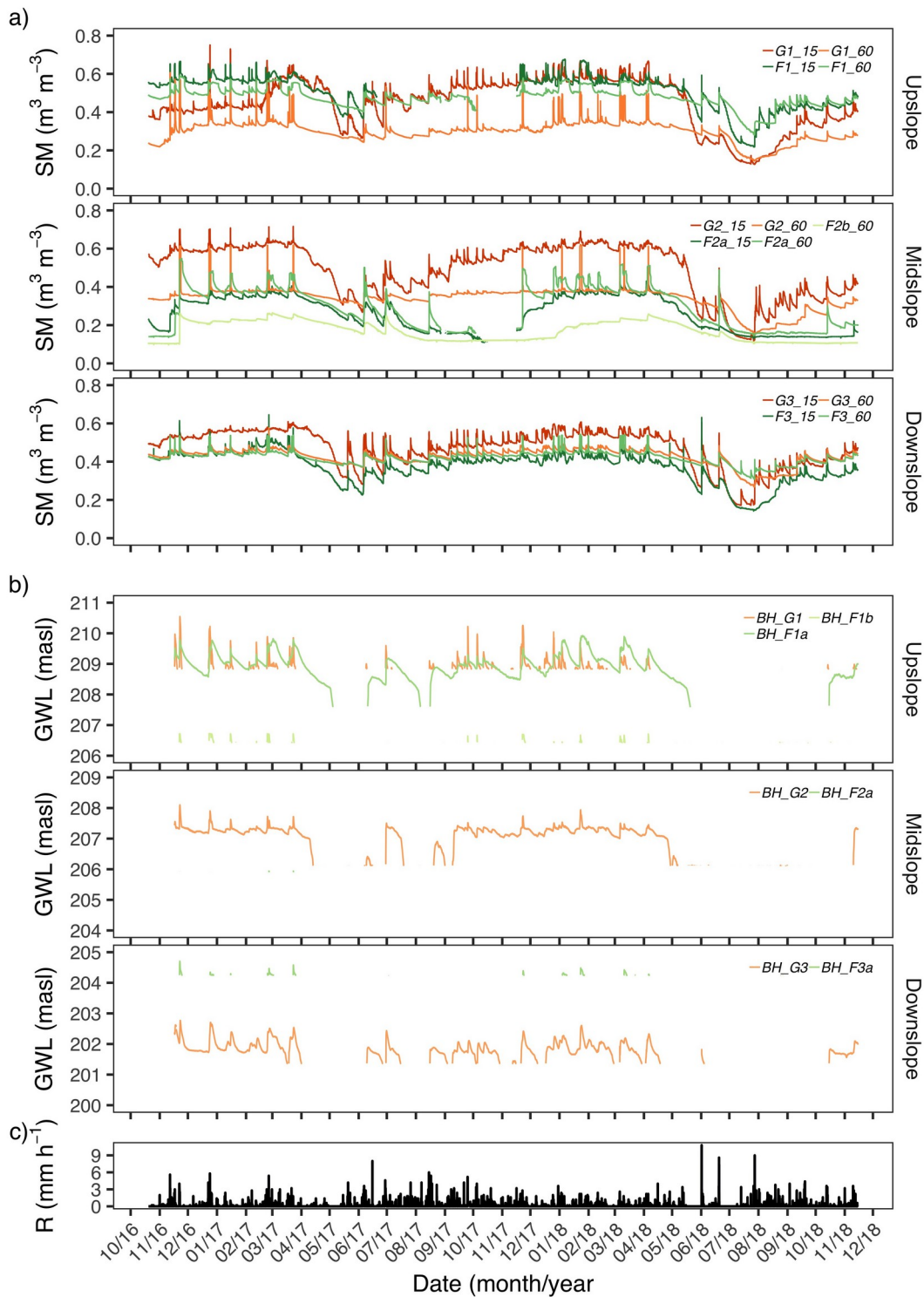
429

430 Soil moisture content in the grassland areas upslope and downslope of the
431 forest strip (F1 and F3 sensors) displayed similar behaviour to those on the
432 grassland transect, with the exception of the 0.6 m depth sensor upslope
433 (F1_60), which had a higher soil moisture content throughout almost the
434 entire time series than the paired grassland sensor (G1_60), possibly due to
435 the location in a shallow topographic depression. The upslope rain gauge had
436 higher daily rainfall than the downslope gauge during the study period (paired
437 t-test, $p < 0.01$), probably due to the prevailing wind direction, but the mean
438 difference was only 0.1 mm d^{-1} .

439

440 **Figure 3: Time series of a) 15-minute soil moisture (SM) and b) 15-**
441 **minute groundwater level (GWL) data from the grassland and forest**

442 **strip transects for the entire study period November 2016-November**
443 **2018. Soil moisture sensor F2b_15 was poorly responsive and**
444 **possibly in an air pocket so data are not shown. Note different y-axis**
445 **scales for GWL data. c) Hourly rainfall data (R) from the upslope rain**
446 **gauge (aggregated from 15-minute data for clarity).**



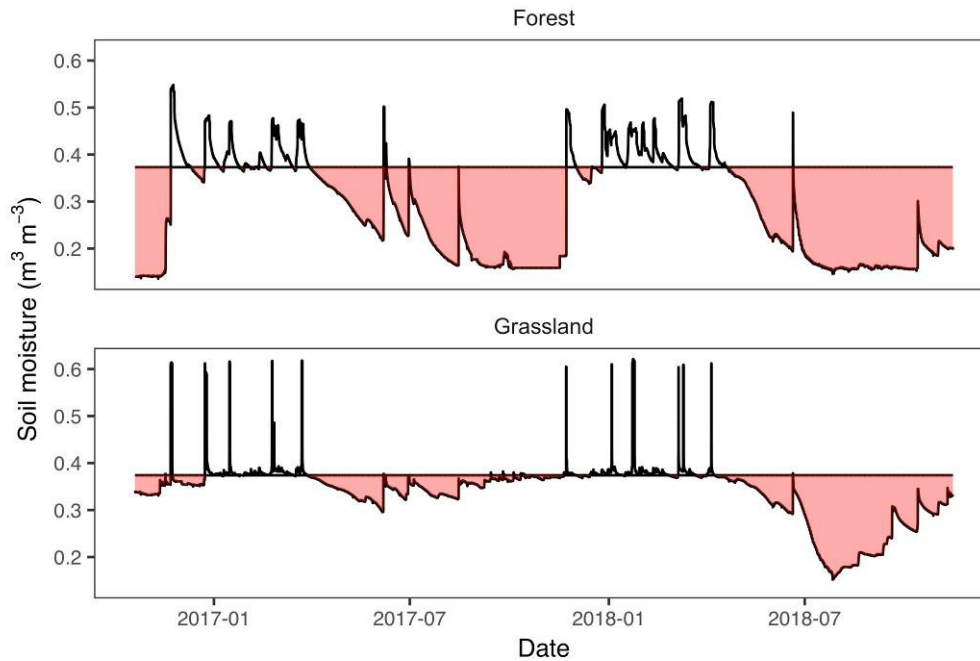
447

448 Over seasonal timescales there was generally more variability in soil moisture
 449 content at 0.15 m depth compared to at 0.6 m depth, apart from in the forest
 450 strip, where seasonal variability was similar in both shallow and deeper soil
 451 depths. This deeper and prolonged drying of the forest soils in summer and

452 autumn has implications for soil water storage potential. For the whole time
453 series, cumulative soil moisture content was 72-75% and 81-96% compared
454 to a baseline of cumulative median winter soil moisture content for all sensors
455 in the forest (F2 sensors) and all sensors on grassland respectively. An
456 example of this contrast between two sensors is shown in Figure 4. Most of
457 the estimated 15% 'additional' storage capacity in the soil beneath the forest
458 strip occurred in the three months September-November. This is likely to be
459 an underestimate of the actual storage, or the additional storage available in
460 winter, because saturation was not observed in the forest soils during the
461 study period.

462

463 **Figure 4: Soil moisture content at 60 cm depth under forest (F2a_60)**
464 **and grassland (G2_60) and for the entire study period compared to**
465 **the baseline of the median winter soil moisture content for each**
466 **sensor (horizontal lines). Highlighted areas are the soil moisture**
467 **deficit in summer/autumn months, indicating the potential soil**
468 **moisture storage.**



469

470 Groundwater data were discontinuous at the depths of all the hillslope
 471 piezometers. A water table was recorded for much of the study period on the
 472 grassland transect and in the upslope part of the forest transect. It was
 473 highest during winter but disappeared from all piezometers during mid-
 474 summer, with a range of over 2 m in some piezometers. In three of the four
 475 piezometers with the most continuous data, the water table showed bi-modal
 476 recession behaviour, with an abrupt drop in water table depth below a
 477 threshold level of 1.87 m below ground level in BH_F1a, 1.50 m in BH_G2 and
 478 2.48 m in BH_G3 (Figure 3). This is indicative of layered geology with large
 479 contrasts in permeability between layers, probably representing the transition
 480 from less permeable glacial till to unconsolidated gravelly head deposits or
 481 weathered rock head.

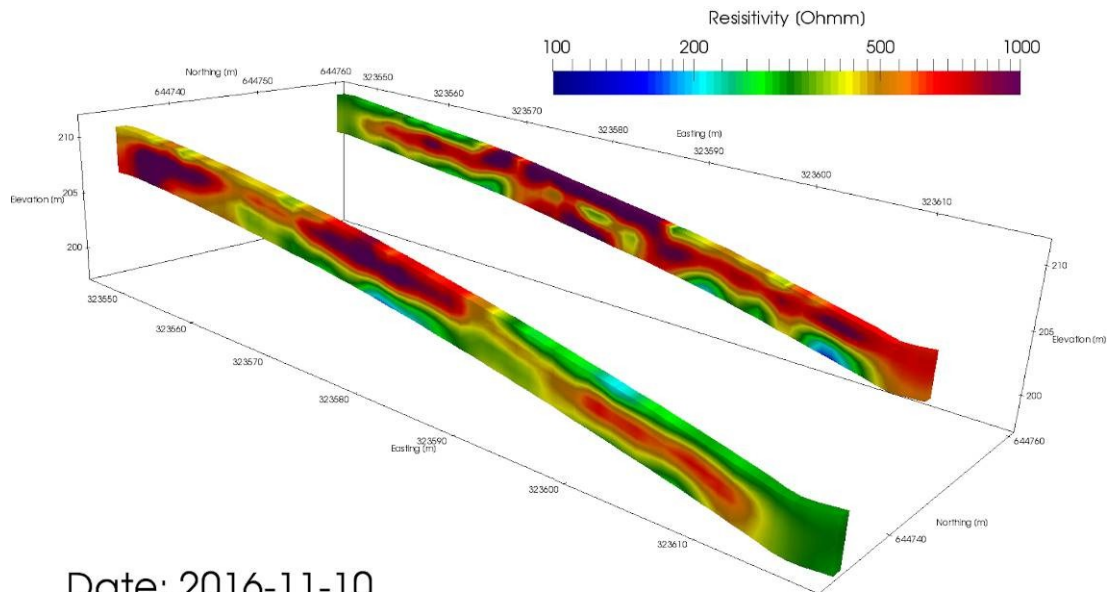
482

483 **3.1.2 ERT survey data**

484 ***Resistivity structure along transects***

485 The resistivity surveys give insights into the geological structure of the
486 hillslope, with a layered structure visible on both transects (an example is
487 given in Figure 5 and the same structures are visible in Figure S2). Outside
488 the forest strip the topmost layer (0-0.5 m) on both transects had lower
489 resistivities in winter and higher resistivities in summer. This layer
490 corresponds with more organic rich soil according to the borehole logs and
491 soil pits, and sits on a much higher resistivity layer (0.5- 1.7 m) that
492 corresponds with glacial till (Table S1, Figure S1). Below 1.7 m depth,
493 resistivities decreased again, probably due to the presence of a water table in
494 many of the grassland areas on both transects, as the borehole logs do not
495 indicate a significant change in geological properties at this depth. The
496 upslope part of the grassland transect differed from other grassland areas,
497 with higher resistivities below a depth of 0.5 m. The resistivity structure was
498 different in the forested area, with less obvious layering and high resistivities
499 to the bottom of the section.

500 **Figure 5: Resistivity cross section for the grassland (foreground) and**
501 **forest (background) transects in November 2016.**



Date: 2016-11-10

502

503

504 ***Resistivity variation with depth and time along transects***

505 The time-lapse ERT data indicate that the variation in resistivity across the
 506 ten surveys generally decreased with depth on both transects and at all slope
 507 locations (Figure 6). However, variability was greater on the forest transect,
 508 particularly to 1.7 m depth within the midslope forest strip area. In this zone
 509 interquartile range (IQR) of the relative resistivities was 4.0-16.8 % for the
 510 forest and 2.5-6.8 % for the adjacent grassland. Within the first 12 m
 511 downslope of the forest, there was also greater variation in relative
 512 resistivities in the top 1.7 m depth compared to the adjacent grassland and
 513 compared to similar locations upslope of the forest. In this zone the IQR of the
 514 relative resistivities was 6.71-12.7 % for the forest and 1.7-10.2 % for the
 515 adjacent grassland (Figure 6).

516

517 The ERT time series data give further insight into the changing seasonal
 518 impact of the forest strip on hillslope subsurface hydrological dynamics along
 519 the hillslope (Figure 7). In the upslope domain, resistivities displayed similar

520 seasonal patterns on both transects. They were higher in the drier summer
521 surveys compared to the autumn, winter and spring surveys, with the
522 amplitude of the changes decreasing with depth, and little variation below 2.5
523 m.

524

525 The largest differences between transects were in the midslope area. The
526 absolute changes in resistivity between surveys were more pronounced in the
527 midslope forest domain than in the grassland, implying more extreme wetting
528 and drying of the subsurface below the forest strip. The forest area also
529 remained more highly resistive later into the year (through the autumn
530 surveys). This effect was minimal below 2.5 m and insignificant below 3.4 m.

531

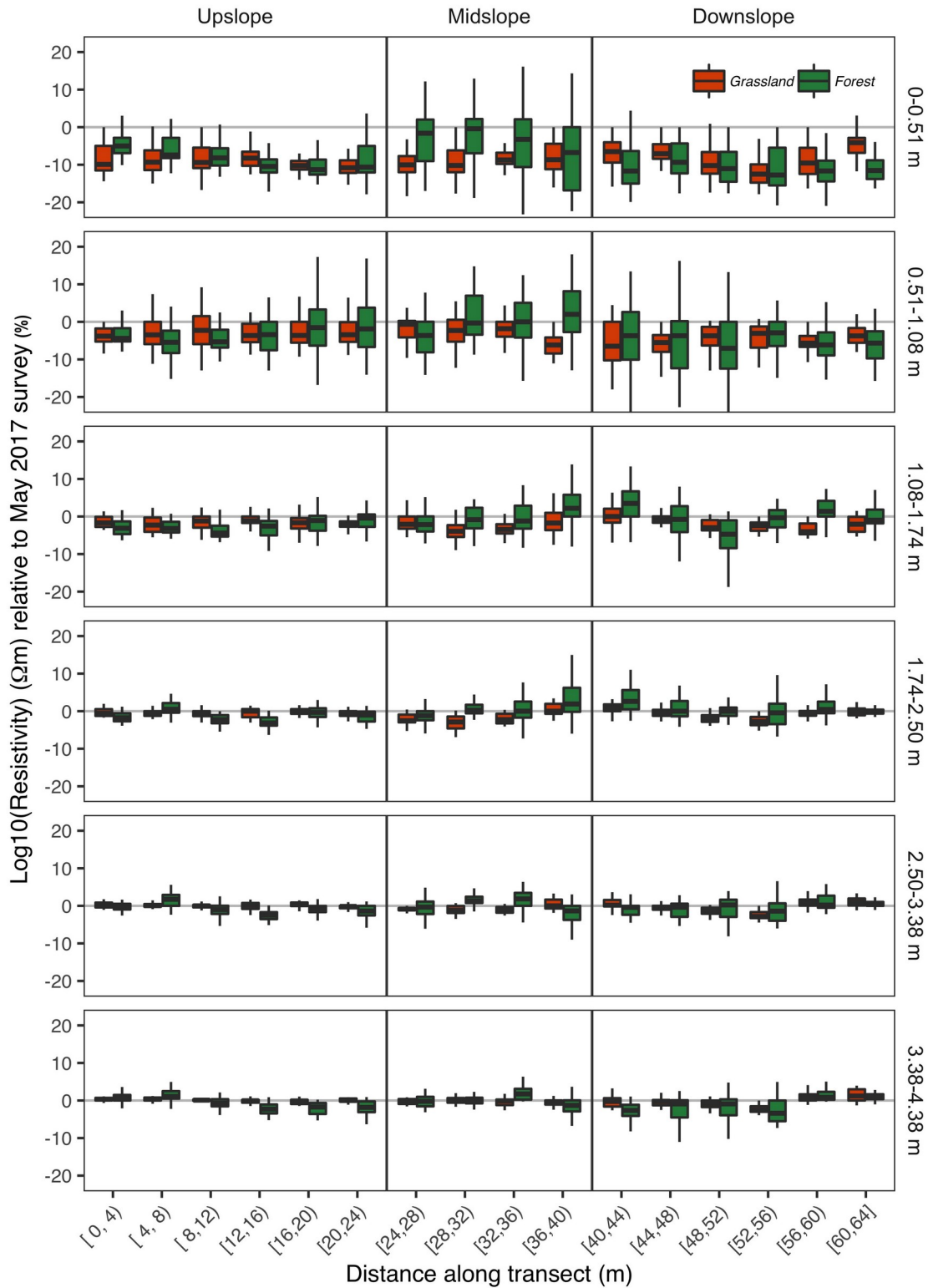
532 The seasonal pattern of changes in resistivity was similar in the downslope
533 domain to the upslope domain, with higher relative resistivities in the summer
534 surveys and lower resistivities in the autumn, winter and spring surveys.

535 There is no indication that the prolonged subsurface drying into the autumn
536 beneath the forested area extended downslope of the forest strip. As in the
537 upslope and midslope domains, the amplitude of seasonal changes decreased
538 with depth on both transects.

539

540 **Figure 6: Resistivity variation at different depths along the two**
541 **transects for the 10 surveys conducted between November 2016 and**
542 **April 2018 relative to the May 2017 survey (horizontal line at 0). The**
543 **forested area is located within the midslope domain. The horizontal**
544 **line inside the box represents the median and the lower and upper**
545 **hinges correspond to the first and third quartiles. The upper and**
546 **lower whiskers depict the largest and smallest values respectively**

547 **within 1.5 * the interquartile range (IQR). Outliers removed for**
548 **clarity. x-axis labels represent range of cells (as distance along the**
549 **transect) used to calculate statistics - e.g. [0,4) indicates the first**
550 **four model cells on the line between 0-1,1-2, 2-3 and 3-4 m.**



551

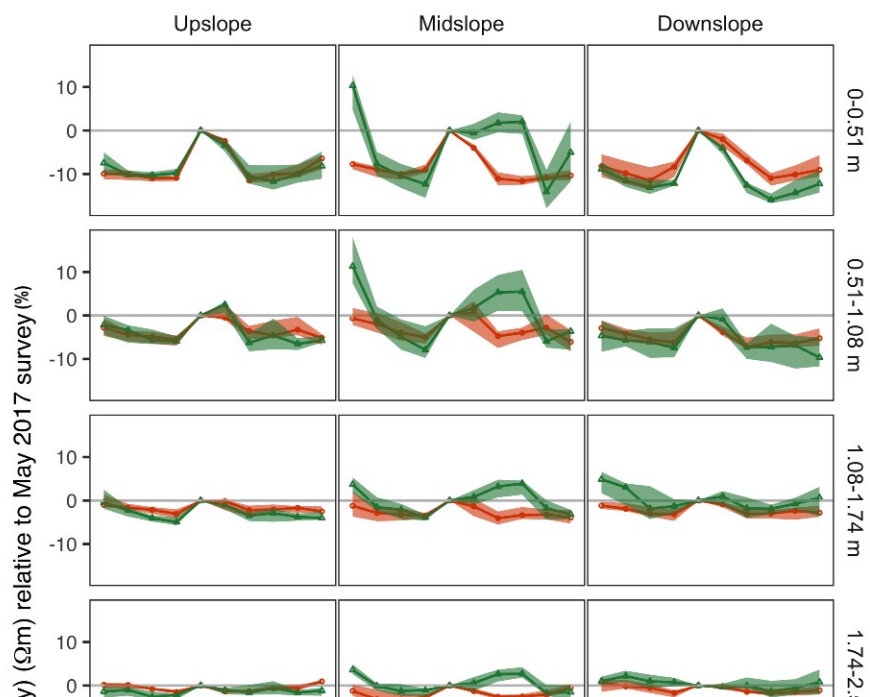
552 **Figure 7: Median resistivities for each transect across different**

553 **domains and depths for the 10 surveys conducted between**

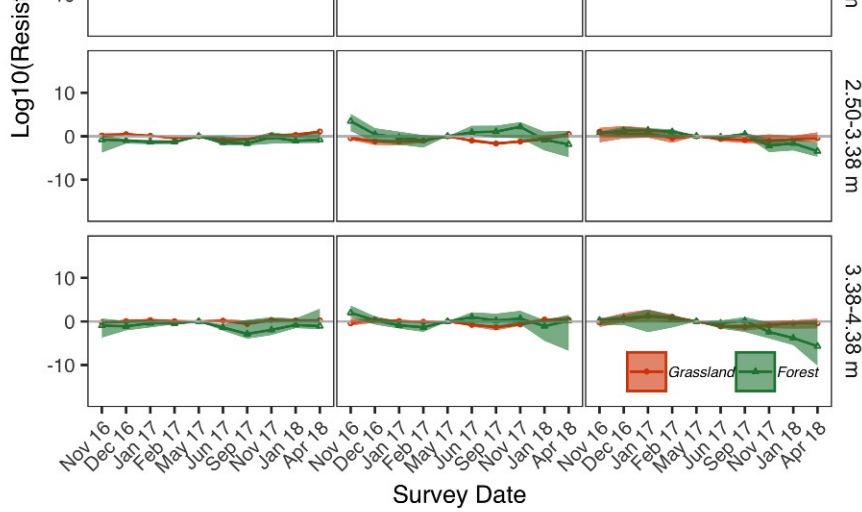
554 **November 2016 and April 2018 relative to the May 2017 survey**

555 **(horizontal line at 0). The forested area is located within the**
556 **midslope domain. Median resistivities for each survey are calculated**
557 **from cells across the whole domain (i.e. 0-24 m for the upslope**
558 **domain, 24-40 m for the midslope domain, and 40-64 m for the**

559 downslope domain). Shading represents 95% confidence intervals.



561
562
563
564
565
566
567
568
569
570
571
572
573
574
575
576
577
578
579
580
581



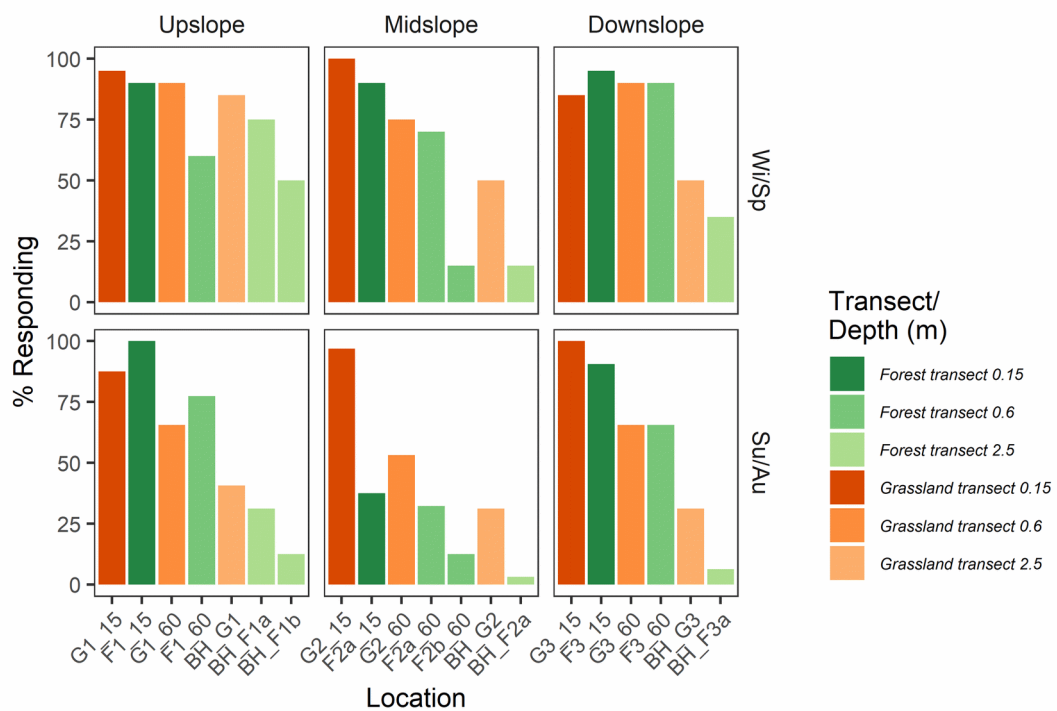
ween

:h in each

:he

groundwater sensors at ~2.5 m depth (Figure 8). However, there were significant differences in the number responding between transects at different locations on the hillslope, when comparing sensors at all depths in each domain. The most significant difference in the number responding was in the midslope domain ($p < 0.001$). 66% of grassland sensors in the midslope domain responded over the 52 events, whilst only 31% responded in the forest strip. Much of the relative decrease in the forest domain was due to fewer of the 0.15 m (particularly in summer) and 2.5 m sensors responding (Figure 8). There was less difference in number responding between the transects in the upslope domain (58% and 74% responded for forest and grassland respectively) and downslope domain (62% and 69% responded for forest and grassland respectively). Some of the difference in the upslope domain can be explained by events not being logged as responses due to soil saturation prior to the event for three events at location F1_60 and one event at F1_15.

582 **Figure 8: Number of sensors responding (%) across all rainfall events**
 583 **(n=52) for all working soil moisture and groundwater sensors at**
 584 **different depths and domains on the forest strip and grassland**
 585 **transects for Winter/Spring (Wi/Sp) and Summer/Autumn (Su/Au)**
 586 **seasons.**

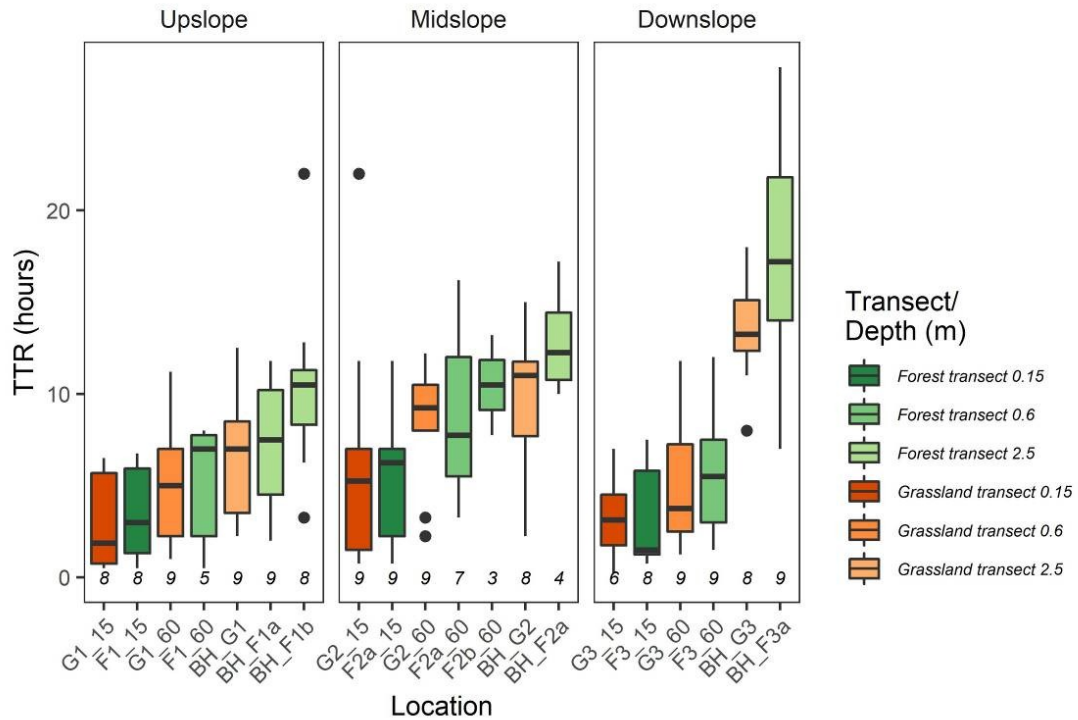


587

588 Comparing data from the nine events when most of the sensors responded,
589 the time taken for sensors to respond (TTR) increased with depth in all
590 domains and there was no significant difference in TTR between forest and
591 grassland transects at any location or depth (Figure 9). However, TTR
592 increased downslope for the piezometers, with significant differences between
593 upslope and downslope locations ($p < 0.05$), but not for the soil moisture
594 sensors (Figure 9). The pairwise comparison of all events ($n=52$) additionally
595 indicates that there were no significant differences in TTR between summer
596 and winter at any location, although summer TTRs were slightly more variable
597 than winter TTRs (Figure S3).

598

599 **Figure 9: Time to response from the start of rainfall (TTR) for the**
600 **different domains and depths on the forest strip and grassland**
601 **transects during nine rainfall events when the borehole downslope of**
602 **the forest responded and the majority of the other soil moisture and**
603 **groundwater sensors responded. The horizontal line inside the box**
604 **represents the median and the lower and upper hinges correspond to**
605 **the first and third quartiles. The upper and lower whiskers depict the**
606 **largest and smallest values respectively within 1.5 * the interquartile**
607 **range (IQR). Numbers in italics show the number of events in which**
608 **sensor responded. Dots are outliers.**



609

610 The time that sensors took to reach peak soil moisture/water table from start
 611 of rainfall (TTPR) and the maximum rise (MR) were much more variable at
 612 individual sensors and between sensors, especially during the subset of nine
 613 events in wetter conditions (Figure S4a). This was mainly due to the rapid
 614 occurrence of saturation in some of the 0.6 m sensors. However, there
 615 appears to be a similar pattern to that seen in the TTR data, of increasing
 616 water table TTPR downslope but no systematic increase in soil moisture TTPR.
 617 The pairwise comparison of all 52 events suggests that TTPR was seasonally
 618 variable, especially in the forested midslope domain. In summer, the TTPR
 619 interquartile range for all forest locations was 13-16 hours, compared to 6-11
 620 hours for the adjacent grassland) (Figure S4b).

621

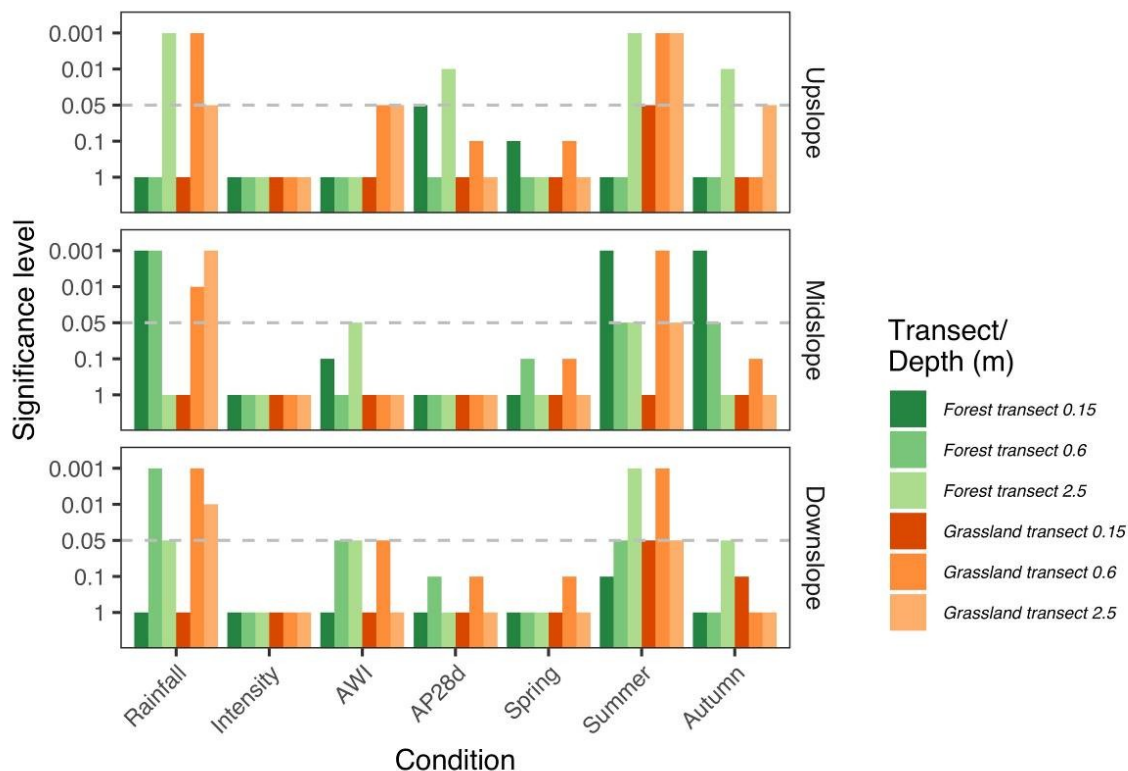
622 **3.2.2 Relationships between event characteristics and**
623 **subsurface hydrology response metrics**

624 Total event rainfall and the 5-day AWI are good predictors of overall number
625 of sensors responding ($p < 0.001$). There are also significant seasonal
626 differences, with the log odds of response much less likely in summer/autumn
627 compared to the winter/spring ($p < 0.001$). Comparison between transects,
628 depths and domains reveals a more complex picture. Total event rainfall and
629 seasonal differences are significant explanatory factors for whether sensors
630 respond to events in most locations (Figure 10). However, event
631 characteristics and seasonal variation in conditions have less impact on the
632 response of the 0.15 m soil moisture sensors, because these respond easily
633 across the whole range of events. The 0.15 m sensor in the forest strip is an
634 exception, where response seems to be significantly affected by total event
635 rainfall and there are significant seasonal differences (in summer/autumn
636 compared to winter/spring) compared to grassland areas. Total event rainfall
637 appears to have a more significant impact on the number of the 0.6 m and
638 2.5 m sensors that respond in most locations, presumably because a
639 threshold level is required for these to respond. The seasonal variation in
640 these deeper sensors is less clear than at shallower levels, but there are
641 similar patterns between 0.6 m sensors on the forest and grassland lines, with
642 significant differences between summer/autumn, compared to winter/spring
643 on the forest transect. These differences are consistent with seasonal
644 changes in soil moisture being more marked in the forest strip, with a later
645 onset of sensor response.

646

647 **Figure 10: Graphical representation of significance levels from**
648 **logistic regression of the number of soil moisture and groundwater**

649 **sensors responding for different transects, domains and depths for**
 650 **different independent variables across all 52 rainfall events. Spring,**
 651 **Summer and Autumn are based on logistic regression comparisons to**
 652 **Winter. Dashed grey line highlights significance level of $p = 0.05$.**



653
 654 Correlation of event characteristics and response metrics at individual
 655 locations showed some significant correlations but no clear pattern could be
 656 identified between transects. Correlation coefficients calculated for data for
 657 all sensors across both transects showed more generally that total event
 658 rainfall appears to be the most important factor controlling MR for both soil
 659 moisture sensors and piezometers. Event intensity also appears to be a
 660 significant control on TTR and TTPR for both soil moisture sensors and
 661 piezometers. Finally, in winter the 5-day AWI appears to be an important
 662 factor in controlling the rate of response of the piezometers and AP28d for the
 663 maximum rise in the soil moisture sensors (Table S4).

664 **4 Discussion**

665 **4.1 Forest influence on soil moisture and groundwater** 666 **dynamics beneath the forest strip**

667 Pronounced differences in subsurface hydrology characteristics and dynamics
668 were identified between the forest strip area and the grassland areas on both
669 transects from the 2-year monitoring programme based on soil moisture,
670 groundwater and time-lapse ERT measurements. These observations have
671 been used to infer the hydrological processes operating in the hillslope and to
672 devise the conceptual model of these described below.

673

674 The forested area had lower absolute but more variable soil moisture content,
675 higher relative ERT resistivities, a considerably lower water table and less
676 event-driven response of subsurface sensors. In the zone above the water
677 table and within the rooting depth of the trees (~ 2.5 m), there were
678 reductions in soil moisture levels and in the numbers of sensors responding
679 during events, that extended later into the autumn compared to the
680 grassland. The ERT data show the same seasonal effects and additionally
681 suggest these were contained within the boundaries of the forest.

682

683 Our conceptual model to explain these findings is shown in Figure 11. We
684 hypothesise that the differences between the grassland (Figure 11a) and the
685 forest strip (Figure 11b) can be attributed to a combination of greater
686 evapotranspiration and canopy interception by trees, and the likely increased
687 infiltration rate of the forest soils and sub-soils due to more extensive rooting
688 systems and their effects on hydraulic conductivity. Studies in the UK have

689 found that interception losses can range between 25 and 50% of
690 precipitation, with greater losses for summer events and the interception
691 fraction decreasing with increasing rainfall (Johnson, 1995). Conifers and
692 broadleaves can also lose an additional 300-390 mm yr⁻¹ through
693 transpiration (Nisbet, 2005). These findings provide indirect evidence to
694 explain the differences in response of the forest sensors between seasons,
695 sporadic responses during larger summer rainfall events and the delayed
696 'wetting up' of the forest soils until the onset of larger rainfall events in the
697 late autumn when some trees had also lost their leaves. Median soil hydraulic
698 conductivities in the forest are likely to range from 42-174 mm h⁻¹, based on
699 results from a study investigating similar hillslopes and land uses in the same
700 catchment, which found that tree rooting systems played a significant role in
701 controlling hydraulic conductivity (Archer et al., 2013). We also found that
702 while there were similarities in the soil matrix and horizon depths under the
703 forest and grassland areas, there were differences in rooting systems, with
704 larger roots and deeper rooting systems in the forest compared to the
705 grassland. These differences in hydraulic conductivity likely contribute to the
706 observed lower absolute soil moisture levels in the forest, higher resistivities
707 and the lower water table.

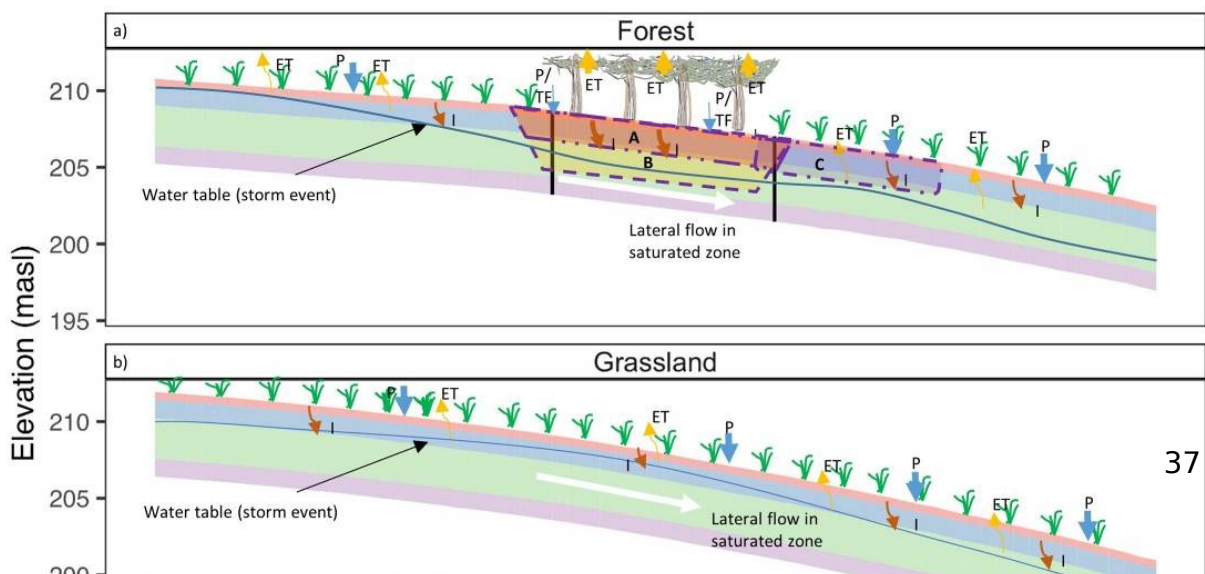
708

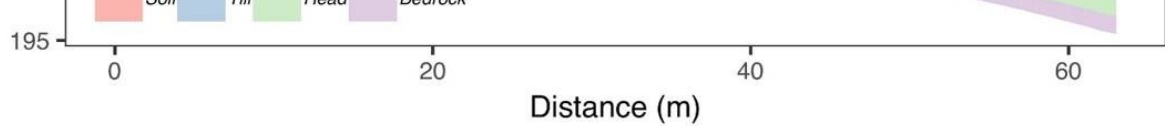
709 At depths greater than 2.5 m there were no significant observable seasonal
710 impacts of the forest on moisture dynamics (Figure 11b). Piezometer data
711 from the rainfall events indicate that the water table was within 2.5 m of the
712 ground surface for the wettest periods in the year, probably attenuating the
713 seasonal variations in resistivity observed at shallower depths. The zone
714 below 2.5 m is also likely to be at the limit of the rooting depths of the trees,

715 reducing their impacts on both evapotranspiration and hydraulic conductivity.
 716 The lower water table in the forest strip compared to the grassland is one of
 717 the most striking differences between the transects (Figure 11). We suggest
 718 that this is due to enhanced hydraulic conductivity within forest soils and sub-
 719 soils, rather than 'pumping' by trees as the effect persists through the winter
 720 when evapotranspiration and interception are greatly reduced.

721 **Figure 11: Conceptual model showing the hillslope with (a) the**
 722 **across-slope forest strip and (b) the grassland transects. The major**
 723 **hydrological fluxes are shown in relation to hillslope, land cover and**
 724 **geological structure, with arrow size relating to the size of the flux.**
 725 **ET: evapotranspiration; P: precipitation; TF: throughfall; I:**
 726 **infiltration. Dashed purple lines in (a) delineate zones of differing**
 727 **moisture dynamics in the forest transect: A) zone within rooting**
 728 **depth of trees (~2.5 m) with greater variability in soil moisture,**
 729 **extended seasonal reduction in soil moisture and reduction in event-**
 730 **driven response of sensors; B) zone below rooting depth of trees and**
 731 **with seasonal water table that attenuates seasonal variation in**
 732 **moisture dynamics observed at shallower depths; and C) zone with**
 733 **greater variation in moisture dynamics (inferred from ERT data) due**
 734 **potentially to deeper unsaturated zone and wind shadow effect close**
 735 **to trees. Depths of zones are not drawn to scale.**

736





737 These results are consistent with studies at the hillslope scale on the effects
738 of forest planting on soil moisture dynamics. Significant increases in hydraulic
739 conductivity in forest soils have been reported (Archer et al., 2013; Carroll et
740 al., 2004; Ghestem et al., 2011; Wheeler et al., 2008), although few studies
741 have examined directly how variations in hydraulic conductivity due to trees
742 affect groundwater levels across hillslopes. Others have demonstrated the
743 seasonal depletion of soil moisture content and groundwater levels due to
744 forest evapotranspiration (Bonell et al., 2010; Greenwood and Buttle, 2014),
745 but there is considerable variability depending on canopy structure, climate
746 and soil and vegetation characteristics (Guswa, 2012). Similar effects of
747 forest planting and removal have been described at the catchment scale,
748 with afforestation/reforestation often leading to a reduction in annual water
749 yield (Bosch and Hewlett, 1982; Brown et al., 2005; Filoso et al., 2017).
750 Recent meta-analysis of the results of catchment studies worldwide has
751 shown the importance of subsurface storage substrate porosity, permeability
752 and unsaturated zone depth, and its relationship to forest cover (Evaristo and
753 McDonnell, 2019) in modulating annual water yield.

754

755 **4.2 Forest influence on downslope soil moisture and** 756 **groundwater dynamics**

757 While the forest strip had measurable impacts on the subsurface hydrological
758 conditions beneath the forest, no significant effects were observed downslope
759 in the zone above the water table (<2.5 m depth). There were no significant
760 differences between transects in long-term median soil moisture content or
761 variability at the downslope soil moisture sensors at 0.15 m and 0.6 m depth.

762 For the same sensors there was no significant difference in rainfall event
763 metrics. In the ERT data, the more extreme seasonal variation and prolonged
764 summer/autumn drying that was observed beneath the forest at depths of
765 <2.5 m was not observed in the hillslope portions downslope of the forest,
766 even in areas very close to the forest (<2 m from the forest boundary). As
767 shown in Figure 11, we suggest that the forest has only limited seasonal
768 influence on shallow moisture dynamics. We attribute this mainly to the
769 dominance of vertical processes (evapotranspiration and drainage) in the
770 unsaturated zone as in other areas of the slope, as well as the continued
771 infiltration and percolation of any surface and shallow subsurface flow as it
772 moves downslope (Klaus and Jackson, 2018).

773

774 These findings notwithstanding, the forest did appear to depress groundwater
775 depths downslope. During the wettest periods, groundwater depths were up
776 to 1.7 m lower downslope of the forest compared to depths upslope of the
777 forest, and up to 1.5 m lower compared to similar locations on the grassland
778 transect. However, there is evidence that groundwater connectivity existed
779 between the areas upslope and downslope of the forest during larger events.
780 Time to response in the 0.15 m and 0.6 m soil moisture sensors was similar
781 at all locations on the slope, but increased downslope for the piezometers.
782 These longer response times downslope than upslope in the piezometers are
783 interpreted as an indication that lateral flow processes from upslope to
784 downslope are more important than vertical infiltration in driving
785 groundwater dynamics in this part of the slope and in moving water down the
786 slope through a connected shallow groundwater system. This implies that
787 the forest does not 'interrupt' lateral downslope water table connectivity

788 during larger events. This is consistent with findings from studies on
789 catchment scale hydrological connectivity and threshold behaviour (Detty
790 and McGuire, 2010a, 2010b; McNamara et al., 2005).

791

792 Lastly, the ERT data show that while median relative resistivities across all
793 surveys were similar between transects in the downslope area, they were
794 more variable at shallow depths (<1.7 m) in the first 12 m downslope of the
795 forest strip, compared to the adjacent grassland and similar locations upslope
796 of the forest strip. This may be indicative of a seasonally variable deeper
797 unsaturated zone in the area immediately downslope of the forest with less
798 attenuation of resistivity due to the seasonal water table. The south-westerly
799 prevailing wind and the north-south orientation of the forest strip means that
800 a rain shadow effect from the forested area could also contribute to such
801 variability. This effect has been observed to extend to ~6 m on to adjacent
802 grassland at sites with similar height trees in the UK, particularly in winter
803 when frontal rainfall is accompanied by stronger winds (Wheater et al., 2008).

804

805 **4.3 Implications for flood risk management**

806 Our study suggests that in temperate environments forest boundary strips
807 could marginally increase catchment storage due to evapotranspirative
808 'pumping' and interception by trees that extends to deeper depths and is
809 more prolonged than in grassland areas. However, our results show that this
810 additional subsurface moisture storage is highly restricted in space to the
811 area in and around the forest itself. This effect is greatest in summer and
812 autumn, so may have a mitigating effect on summer flood events, but
813 additional storage capacity is likely to be limited in winter and spring. Such

814 effects are also likely to vary with forest type and age, as discussed in other
815 studies (Archer et al., 2013; Chandler et al., 2018; Jipp et al., 1998). Given
816 that flood events commonly have higher frequencies in summer in small
817 catchments in Scotland (Black and Werritty, 1997) and in the immediate
818 region of this study (Masson, 2019), additional subsurface moisture storage
819 provided in summer by forest strips may provide some benefit depending on
820 storm characteristics and antecedent conditions.

821

822 At the storm event timescale, our results suggest that forest strips locally
823 decrease the responsiveness of soils and groundwater beneath the forest
824 strip to rainfall events, especially in summer/autumn. During larger rainfall
825 events and in winter, forest soils respond similarly to rainfall events and at
826 similar rates as grassland, but appear to saturate less frequently, suggesting
827 that forest strips could reduce runoff through combined effects of intra-event
828 evaporation and more rapid drainage to the subsurface. This is aligned with
829 reported increased hydraulic conductivity and porosity in soils below forest
830 strips (Carroll et al., 2004; Wheeler et al., 2008).

831

832 From this study, the spatial influence of forest strips appears to be slightly
833 larger than their width, with some downslope depression observed in soil
834 moisture content and groundwater levels. In slopes with much less
835 permeable soils or compacted soils, the forest may act more like a “French
836 drain”, channelling water into deeper layers. However, the effectiveness of
837 such a system would be limited by the connectivity of the ‘drain’ to deeper,
838 more permeable substrate, or to more permeable areas laterally, and to the
839 permeability of soils/geology downslope. On its own the limited storage

840 capacity of the strip would be quickly overwhelmed if surrounded by a less
841 permeable system. This highlights the highly context-specific nature of the
842 impacts of forest strips on subsurface moisture storage and on the
843 attenuation effects of increases in hydraulic conductivity.

844

845 The role of water table connectivity and its links to threshold behaviour in
846 catchment response is increasingly recognised in the hydrological literature
847 (Bracken et al., 2013; Detty and McGuire, 2010a). This study suggests that
848 the forest strip has little impact on groundwater connectivity during larger
849 events, implying that similar upland landscapes with fragmented forest strips
850 might have limited impact on groundwater dynamics at the event timescale
851 and in wetter periods. There is need for further investigation to assess
852 whether there are optimal soil and geological conditions, and extents and
853 locations of forest cover that might have a larger influence at the catchment
854 scale, as has been suggested in other environments (Ilstedt et al., 2016).

855

856 **4.4 Conclusions**

857 Forest strips are being used around the world for reduction of flood risk.
858 Nevertheless, our knowledge of how forest strips impact runoff in general and
859 local- and down-gradient hydrological conditions, is still poor. This study
860 examined the impact of an across-slope forest strip on sub-surface soil
861 moisture and groundwater dynamics. We found that an increase in soil
862 moisture storage potential associated with the forest strip was highly
863 seasonal and did not extend much beyond the forest strip itself. In this
864 temperate climate, during wetter winter periods, when widespread runoff is
865 typically highest, isolated strips of forest like the one we studied are likely to

866 have only a marginal impact on sub-surface moisture storage. However, in
867 specific contexts, such as lower magnitude events or intense summer storms,
868 forest strips could locally reduce catchment responsiveness to storm events.
869 This study only considered sub-surface processes; the impacts of forest strips
870 on surface runoff, for example through increased roughness and infiltration,
871 could be greater.

872

873 Our study showed the utility of time-lapse ERT for extrapolating findings from
874 point-based measurements along hillslopes and to greater depths in terrain
875 that is difficult to instrument invasively. ERT helped to show the larger, longer
876 and deeper seasonal changes in soil moisture in the forest compared to
877 adjacent grassland, as well as providing insight into the lateral variability of
878 moisture changes within the transects. Higher frequency ERT data that is now
879 available at daily or sub-daily time-steps (Chambers et al., 2014) would be a
880 useful extension to this study to further understanding of subsurface
881 hydrological dynamics at the storm event scale.

882 **Acknowledgements**

883 We would like to thank the landowner for giving us access to the site and the
884 Tweed Forum for their help in identifying suitable sites within the wider
885 Eddleston Natural Flood Management project. We would also like to thank
886 Robert Fairhurst, Adam Francis, Anthony Newton, Kirsty Shorter, Heiko Buxel
887 and Jez Everest for their help with fieldwork.

888

889 **Funding:** This work was supported by L. Peskett's NERC E³ DTP /BGS BUFI
890 PhD studentship at the University of Edinburgh, UK (grant number
891 NE/L002558/1) and associated NERC Research Experience Placement grant to

892 R. Fairhurst; a University of Edinburgh Innovation Initiative Grant (grant
893 number GR002682); a SAGES Postdoctoral & Early Career Researcher
894 Exchange (PECRE) grant supporting collaboration with J. McDonnell; and in-
895 kind contributions and loan of equipment from the School of GeoSciences,
896 University of Edinburgh and BGS Edinburgh and Keyworth offices.
897

898 **References**

- 899 Archer, N.A.L., Bonell, M., Coles, N., MacDonald, A.M., Auton, C.A., Stevenson,
900 R., 2013. Soil characteristics and landcover relationships on soil
901 hydraulic conductivity at a hillslope scale: A view towards local flood
902 management. *J. Hydrol.* 497, 208-222.
903 <https://doi.org/10.1016/j.jhydrol.2013.05.043>
- 904 ASTM international, 2004. Standard test methods for particle-size distribution
905 (gradation) of soils using sieve analysis. ASTM International.
- 906 Auton, C., 2011. Eddleston Water Catchment, Superficial Geology, 1: 25 000
907 Scale.
- 908 Bachmair, S., Weiler, M., 2012. Hillslope characteristics as controls of
909 subsurface flow variability. *Hydrol. Earth Syst. Sci.* 16, 3699-3715.
- 910 Ball, D.F., 1964. Loss-on-ignition as an estimate of organic matter and organic
911 carbon in non-calcareous soils. *J. Soil Sci.* 15, 84-92.
912 <https://doi.org/10.1111/j.1365-2389.1964.tb00247.x>
- 913 Black, A.R., Werritty, A., 1997. Seasonality of flooding: a case study of North
914 Britain. *J. Hydrol.* 195, 1-25. [https://doi.org/10.1016/S0022-](https://doi.org/10.1016/S0022-1694(96)03264-7)
915 [1694\(96\)03264-7](https://doi.org/10.1016/S0022-1694(96)03264-7)
- 916 Bonell, M., Purandara, B.K., Venkatesh, B., Krishnaswamy, J., Acharya, H.A.K.,
917 Singh, U.V., Jayakumar, R., Chappell, N., 2010. The impact of forest use
918 and reforestation on soil hydraulic conductivity in the Western Ghats of
919 India: Implications for surface and sub-surface hydrology. *J. Hydrol.*
920 391, 47-62. <https://doi.org/10.1016/j.jhydrol.2010.07.004>

921 Bosch, J.M., Hewlett, J.D., 1982. A review of catchment experiments to
922 determine the effect of vegetation changes on water yield and
923 evapotranspiration. *J. Hydrol.* 55, 3–23.

924 Bracken, L.J., Wainwright, J., Ali, G.A., Tetzlaff, D., Smith, M.W., Reaney, S.M.,
925 Roy, A.G., 2013. Concepts of hydrological connectivity: Research
926 approaches, pathways and future agendas. *Earth-Sci. Rev.* 119, 17–34.
927 <https://doi.org/10.1016/j.earscirev.2013.02.001>

928 Brown, A.E., Zhang, L., McMahon, T.A., Western, A.W., Vertessy, R.A., 2005. A
929 review of paired catchment studies for determining changes in water
930 yield resulting from alterations in vegetation. *J. Hydrol.* 310, 28–61.
931 <https://doi.org/10.1016/j.jhydrol.2004.12.010>

932 Brunet, P., Clément, R., Bouvier, C., 2010. Monitoring soil water content and
933 deficit using Electrical Resistivity Tomography (ERT) – A case study in
934 the Cevennes area, France. *J. Hydrol.* 380, 146–153.
935 <https://doi.org/10.1016/j.jhydrol.2009.10.032>

936 Carroll, Z.L., Bird, S.B., Emmett, B.A., Reynolds, B., Sinclair, F.L., 2004. Can
937 tree shelterbelts on agricultural land reduce flood risk? *Soil Use Manag.*
938 20, 357–359. <https://doi.org/10.1111/j.1475-2743.2004.tb00381.x>

939 Cassiani, G., Godio, A., Stocco, S., Villa, A., Deiana, R., Frattini, P., Rossi, M.,
940 2009. Monitoring the hydrologic behaviour of a mountain slope via
941 time-lapse electrical resistivity tomography. *Near Surf. Geophys.* 7,
942 475–486.

943 Cassiani, G., Ursino, N., Deiana, R., Vignoli, G., Boaga, J., Rossi, M., Perri, M.T.,
944 Blaschek, M., Duttmann, R., Meyer, S., Ludwig, R., Soddu, A., Dietrich,

945 P., Werban, U., 2012. Noninvasive Monitoring of Soil Static
946 Characteristics and Dynamic States: A Case Study Highlighting
947 Vegetation Effects on Agricultural Land. *Vadose Zone J.* 11.
948 <https://doi.org/10.2136/vzj2011.0195>

949 Chambers, J.E., Gunn, D.A., Wilkinson, P.B., Meldrum, P.I., Haslam, E.,
950 Holyoake, S., Kirkham, M., Kuras, O., Merritt, A., Wragg, J., 2014. 4D
951 electrical resistivity tomography monitoring of soil moisture dynamics
952 in an operational railway embankment. *Near Surf. Geophys.* 12, 61–72.
953 <https://doi.org/10.3997/1873-0604.2013002>

954 Chandler, K.R., Stevens, C.J., Binley, A., Keith, A.M., 2018. Influence of tree
955 species and forest land use on soil hydraulic conductivity and
956 implications for surface runoff generation. *Geoderma* 310, 120–127.
957 <https://doi.org/10.1016/j.geoderma.2017.08.011>

958 Crow, P., 2005. The Influence of Soils and Species on Tree Root Depth,
959 Information note. Forestry Commission, Edinburgh.

960 Dadson, S., Hall, J., Murgatroyd, A., Acreman, M., Bates, P., Beven, K.,
961 Heathwaite, L., Holden, J., Holman, I., Lane, S., O'Connell, E., Penning-
962 Rowsell, E., Reynard, N., Sear, D., Thorne, C., Wilby, R., 2017. A
963 restatement of the natural science evidence concerning catchment-
964 based 'natural' flood management in the UK. *Proc. R. Soc. A.* 473,
965 20160706. <https://doi.org/10.1098/rspa.2016.0706>

966 Detty, J.M., McGuire, K.J., 2010a. Topographic controls on shallow
967 groundwater dynamics: implications of hydrologic connectivity
968 between hillslopes and riparian zones in a till mantled catchment.
969 *Hydrol. Process.* 24, 2222–2236. <https://doi.org/10.1002/hyp.7656>

970 Detty, J.M., McGuire, K.J., 2010b. Threshold changes in storm runoff
971 generation at a till-mantled headwater catchment. *Water Resour. Res.*
972 46, W07525. <https://doi.org/10.1029/2009wr008102>

973 Environment Agency, 2018. *Working with Natural Processes – Evidence*
974 *Directory* (No. SC150005). Environment Agency, Bristol.

975 Evaristo, J., McDonnell, J.J., 2019. Global analysis of streamflow response to
976 forest management. *Nature*. 570, 455–461.
977 <https://doi.org/10.1038/s41586-019-1306-0>

978 Filoso, S., Bezerra, M.O., Weiss, K.C.B., Palmer, M.A., 2017. Impacts of forest
979 restoration on water yield: A systematic review. *PLOS ONE* 12,
980 e0183210. <https://doi.org/10.1371/journal.pone.0183210>

981 Fraser, A.I., Gardiner, J.B.H., 1967. *Rooting and Stability in Sitka Spruce* (No.
982 40), Forestry Commission Bulletin. Forestry Commission, Farnham.

983 Fu, B.-J., Wang, Y.-F., Lu, Y.-H., He, C.-S., Chen, L.-D., Song, C.-J., 2009. The
984 effects of land-use combinations on soil erosion: a case study in the
985 Loess Plateau of China. *Prog. Phys. Geogr. Earth Environ.* 33, 793–804.
986 <https://doi.org/10.1177/0309133309350264>

987 Garcia-Montiel, D.C., Coe, M.T., Cruz, M.P., Ferreira, J.N., da Silva, E.M.,
988 Davidson, E.A., 2008. Estimating Seasonal Changes in Volumetric Soil
989 Water Content at Landscape Scales in a Savanna Ecosystem Using
990 Two-Dimensional Resistivity Profiling. *Earth Interact.* 12, 1–25.
991 <https://doi.org/10.1175/2007EI238.1>

992 Ghestem, M., Sidle, R.C., Stokes, A., 2011. The Influence of Plant Root
993 Systems on Subsurface Flow: Implications for Slope Stability.
994 BioScience 61, 869–879. <https://doi.org/10.1525/bio.2011.61.11.6>

995 Graham, M.T., Ball, D.F., Ó Dochartaigh, B.É., MacDonald, A.M., 2009. Using
996 transmissivity, specific capacity and borehole yield data to assess the
997 productivity of Scottish aquifers. Q. J. Eng. Geol. Hydrogeol. 42, 227–
998 235. <https://doi.org/10.1144/1470-9236/08-045>

999 Granger, R.J., Gray, D.M., 1989. Evaporation from natural nonsaturated
1000 surfaces. J. Hydrol. 111, 21–29. [https://doi.org/10.1016/0022-](https://doi.org/10.1016/0022-1694(89)90249-7)
1001 [1694\(89\)90249-7](https://doi.org/10.1016/0022-1694(89)90249-7)

1002 Greenwood, W.J., Buttle, J.M., 2014. Effects of reforestation on near-surface
1003 saturated hydraulic conductivity in a managed forest landscape,
1004 southern Ontario, Canada. Ecohydrology 7, 45–55.
1005 <https://doi.org/10.1002/eco.1320>

1006 Guswa, A.J., 2012. Canopy vs. Roots: Production and Destruction of Variability
1007 in Soil Moisture and Hydrologic Fluxes. Vadose Zone J. 11, 1–13.
1008 <https://doi.org/doi:10.2136/vzj2011.0159>

1009 Haddad, N.M., Brudvig, L.A., Clobert, J., Davies, K.F., Gonzalez, A., Holt, R.D.,
1010 Lovejoy, T.E., Sexton, J.O., Austin, M.P., Collins, C.D., Cook, W.M.,
1011 Damschen, E.I., Ewers, R.M., Foster, B.L., Jenkins, C.N., King, A.J.,
1012 Laurance, W.F., Levey, D.J., Margules, C.R., Melbourne, B.A., Nicholls,
1013 A.O., Orrock, J.L., Song, D.-X., Townshend, J.R., 2015. Habitat
1014 fragmentation and its lasting impact on Earth’s ecosystems. Sci. Adv.
1015 1, e1500052. <https://doi.org/10.1126/sciadv.1500052>

1016 Hewlett, J.D., Hibbert, A.R., 1967. Factors affecting the response of small
1017 watersheds to precipitation in humid areas, in: Sopper, W.E., Lull, H.W.
1018 (Eds.), *Forest Hydrology*. Pergamon Press, New York, pp. 275–90.

1019 Hornbeck, J.W., Pierce, R.S., Federer, C.A., 1970. Streamflow changes after
1020 forest clearing in New England. *Water Resour. Res.* 6, 1124–1132.

1021 Ilstedt, U., Bargués Tobella, A., Bazié, H.R., Bayala, J., Verbeeten, E., Nyberg,
1022 G., Sanou, J., Benegas, L., Murdiyarsa, D., Laudon, H., Sheil, D.,
1023 Malmer, A., 2016. Intermediate tree cover can maximize groundwater
1024 recharge in the seasonally dry tropics. *Sci. Rep.* 6, 21930.
1025 <https://doi.org/10.1038/srep21930>

1026 Jackson, B.M., Wheeler, H.S., McIntyre, N.R., Chell, J., Francis, O.J., Frogbrook,
1027 Z., Marshall, M., Reynolds, B., Solloway, I., 2008. The impact of upland
1028 land management on flooding: insights from a multiscale experimental
1029 and modelling programme. *J. Flood Risk Manag.* 1, 71–80.
1030 <https://doi.org/10.1111/j.1753-318X.2008.00009.x>

1031 Jayawickreme, D.H., Van Dam, R.L., Hyndman, D.W., 2008. Subsurface
1032 imaging of vegetation, climate, and root-zone moisture interactions.
1033 *Geophys. Res. Lett.* 35. <https://doi.org/10.1029/2008GL034690>

1034 Jipp, P.H., Nepstad, D.C., Cassel, D.K., de Carvalho, C.R., 1998. Deep Soil
1035 Moisture Storage and Transpiration in Forests and Pastures of
1036 Seasonally-Dry Amazonia, in: Markham, A. (Ed.), *Potential Impacts of
1037 Climate Change on Tropical Forest Ecosystems*. Springer Netherlands,
1038 Dordrecht, pp. 255–272. https://doi.org/10.1007/978-94-017-2730-3_11

- 1039 Johnson, R.C., 1995. Effects of upland afforestation on water resources - The
1040 Balquhiddy Experiment 1981-1991, IH Report No. 116 (2nd edition).
1041 Institute of Hydrology, Crowmarsh Gifford.
- 1042 Klaus, J., Jackson, C.R., 2018. Interflow Is Not Binary: A Continuous Shallow
1043 Perched Layer Does Not Imply Continuous Connectivity. *Water Resour.*
1044 *Res.* 54, 5921–5932. <https://doi.org/10.1029/2018WR022920>
- 1045 Kohler, M.A., Linsley, R.K., 1951. Predicting the runoff from storm rainfall. US
1046 Department of Commerce, Weather Bureau, Washington DC.
- 1047 Lane, S.N., 2017. Natural flood management. *Wiley Interdiscip. Rev. Water* 4,
1048 e1211. <https://doi.org/10.1002/wat2.1211>
- 1049 Liu, J., Gao, G., Wang, S., Jiao, L., Wu, X., Fu, B., 2018. The effects of
1050 vegetation on runoff and soil loss: Multidimensional structure analysis
1051 and scale characteristics. *J. Geogr. Sci.* 28, 59–78.
1052 <https://doi.org/10.1007/s11442-018-1459-z>
- 1053 Loke, M.H., Chambers, J.E., Rucker, D.F., Kuras, O., Wilkinson, P.B., 2013.
1054 Recent developments in the direct-current geoelectrical imaging
1055 method. *J. Appl. Geophys.* 95, 135–156.
1056 <https://doi.org/10.1016/j.jappgeo.2013.02.017>
- 1057 Lunka, P., Patil, S.D., 2016. Impact of tree planting configuration and grazing
1058 restriction on canopy interception and soil hydrological properties:
1059 implications for flood mitigation in silvopastoral systems. *Hydrol.*
1060 *Process.* 30, 945–958. <https://doi.org/10.1002/hyp.10630>
- 1061 MacDonald, A.M., Maurice, L., Dobbs, M.R., Reeves, H.J., Auton, C.A., 2012.
1062 Relating in situ hydraulic conductivity, particle size and relative density

1063 of superficial deposits in a heterogeneous catchment. *J. Hydrol.* 434–
1064 435, 130–141. <https://doi.org/10.1016/j.jhydrol.2012.01.018>

1065 Marshall, M.R., Francis, O.J., Frogbrook, Z.L., Jackson, B.M., McIntyre, N.,
1066 Reynolds, B., Solloway, I., Wheater, H.S., Chell, J., 2009. The impact of
1067 upland land management on flooding: results from an improved
1068 pasture hillslope. *Hydrol. Process.* 23, 464–475.

1069 Masson, J., 2019. How do barometric seiche waves affect historic and current
1070 flood magnitude and seasonality at Portmore and Talla reservoirs?
1071 (Unpublished BSc dissertation). School of Social Sciences, University of
1072 Dundee, Dundee.

1073 McNamara, J.P., Chandler, D., Seyfried, M., Achet, S., 2005. Soil moisture
1074 states, lateral flow, and streamflow generation in a semi-arid,
1075 snowmelt-driven catchment. *Hydrol. Process.* 19, 4023–4038.

1076 Nisbet, T.R., 2005. Water use by trees, Information Note No. FCIN065.
1077 Forestry Commission, Edinburgh.

1078 Ó Dochartaigh, B.É., Archer, N.A.L., Peskett, L., MacDonald, A.M., Black, A.R.,
1079 Auton, C.A., Merritt, J.E., Goody, D.C., Bonell, M., 2018. Geological
1080 structure as a control on floodplain groundwater dynamics. *Hydrogeol.*
1081 *J.* 27, 703–716. <https://doi.org/10.1007/s10040-018-1885-0>

1082 Ó Dochartaigh, B.É., MacDonald, A.M., Fitzsimons, V., Ward, R., 2015.
1083 Scotland’s aquifers and groundwater bodies (Open Report No.
1084 OR/15/028). British Geological Survey, Keyworth.

1085 Reaney, S.M., Bracken, L.J., Kirkby, M.J., 2014. The importance of surface
1086 controls on overland flow connectivity in semi-arid environments:

1087 results from a numerical experimental approach. *Hydrol. Process.* 28,
1088 2116–2128. <https://doi.org/10.1002/hyp.9769>

1089 Scherrer, S., Naef, F., Faeh, A.O., Cordery, I., 2007. Formation of runoff at the
1090 hillslope scale during intense precipitation. *Hydrol Earth Syst Sci*, 11,
1091 907-922.

1092 Soulsby, C., Dick, J., Scheliga, B., Tetzlaff, D., 2017. Taming the flood—How
1093 far can we go with trees? *Hydrol. Process.* 31, 3122–3126.
1094 <https://doi.org/10.1002/hyp.11226>

1095 Swank, W.T., Swift Jr, L.W., Douglass, J.E., 1988. Streamflow changes
1096 associated with forest cutting, species conversions, and natural
1097 disturbances, in: Swank, W.T., Crossley Jr, D.A. (Eds.), *Forest Hydrology
1098 and Ecology at Coweeta*. Springer-Verlag, New York, pp. 297–312.

1099 Tromp-van Meerveld, H.J., McDonnell, J.J., 2006. Threshold relations in
1100 subsurface stormflow: 2. The fill and spill hypothesis. *Water Resour.
1101 Res.* 42, W02411. [0.1029/2004WR003800](https://doi.org/10.1029/2004WR003800)

1102 Tweed Forum, 2019. The Eddleston Water Project [WWW Document]. [https://
1103 tweedforum.org/our-work/projects/the-eddleston-water-project/](https://tweedforum.org/our-work/projects/the-eddleston-water-project/)

1104 Uchida, T., McDonnell, J.J., Asano, Y., 2006. Functional intercomparison of
1105 hillslopes and small catchments by examining water source, flowpath
1106 and mean residence time. *J. Hydrol.* 327, 627–642.
1107 <https://doi.org/10.1016/j.jhydrol.2006.02.037>

1108 Uchida, T., Tromp-van Meerveld, I., McDonnell, J.J., 2005. The role of lateral
1109 pipe flow in hillslope runoff response: an intercomparison of non-linear

1110 hillslope response. *J. Hydrol.* 311, 117–133.
1111 <https://doi.org/10.1016/j.jhydrol.2005.01.012>

1112 Wenninger, J., Uhlenbrook, S., Tilch, N., Leibundgut, C., 2004. Experimental
1113 evidence of fast groundwater responses in a hillslope/floodplain area in
1114 the Black Forest Mountains, Germany. *Hydrol. Process.* 18, 3305–3322.
1115 <https://doi.org/10.1002/hyp.5686>

1116 Werritty, A., Ball, T., Spray, C., Bonell, M., Rouillard, J., Archer, N.A.L., 2010.
1117 Restoration strategy: Eddleston Water Scoping Study. University of
1118 Dundee, Dundee.

1119 Wheeler, H., Evans, E., 2009. Land use, water management and future flood
1120 risk. *Land Use Policy* 26, S251–S264.

1121 Wheeler, H., Reynolds, B., McIntyre, N., Marshall, M., Jackson, B., Frogbrook,
1122 Z., Solloway, I., Francis, O., Chell, J., 2008. Impacts of upland land
1123 management on flood risk: Multi-scale modelling methodology and
1124 results from the Pontbren experiment (No. UR 16), FRMRC Research
1125 Report. University of Manchester, Manchester.
1126 [https://nora.nerc.ac.uk/id/eprint/5890/1/ur16_impacts_upland_land_ma](https://nora.nerc.ac.uk/id/eprint/5890/1/ur16_impacts_upland_land_management_wp2_2_v1_0.pdf)
1127 [nagement_wp2_2_v1_0.pdf](https://nora.nerc.ac.uk/id/eprint/5890/1/ur16_impacts_upland_land_management_wp2_2_v1_0.pdf)

1128 Ziegler, A.D., Giambelluca, T.W., Tran, L.T., Vana, T.T., Nullet, M.A., Fox, J.,
1129 Vien, T.D., Pinthong, J., Maxwell, J.F., Evett, S., 2004. Hydrological
1130 consequences of landscape fragmentation in mountainous northern
1131 Vietnam: evidence of accelerated overland flow generation. *J. Hydrol.*
1132 287, 124–146. <https://doi.org/10.1016/j.jhydrol.2003.09.027>

1133 Zimmermann, B., Elsenbeer, H., De Moraes, J.M., 2006. The influence of land-
1134 use changes on soil hydraulic properties: Implications for runoff
1135 generation. For. Ecol. Manag. 222, 29-38.
1136 <https://doi.org/10.1016/j.foreco.2005.10.070>
1137
1138

1139 **Supplementary Information on:**
1140
1141 **The impact of across-slope forest strips on**
1142 **hillslope subsurface hydrological dynamics**

1143

1144 Leo Peskett^{a,b,*}

1145 Alan MacDonald^b

1146 Kate Heal^a

1147 Jeffrey J. McDonnell^{c,d}

1148 Jon Chambers^e

1149 Sebastian Uhlemann^{e,2}

1150 Kirsty Upton^b

1151 Andrew Black^f

1152

1153 ^aUniversity of Edinburgh, School of GeoSciences, Crew Building, Alexander
1154 Crum Brown Road, Edinburgh EH9 3FF, United Kingdom leo.peskett@ed.ac.uk

1155 ^bBritish Geological Survey, The Lyell Centre, Research Avenue South,
1156 Edinburgh EH14 4AP, United Kingdom

37 ² Present address: Earth & Environmental Sciences, Lawrence Berkeley National
38 Laboratory, Berkeley, CA 94720, USA

1157 ^eGlobal Institute for Water Security, School of Environment and Sustainability,
1158 University of Saskatchewan, Saskatoon SK S7N 3H5, Canada

1159 ^dSchool of Geography, Earth and Environmental Sciences, University of
1160 Birmingham, Birmingham B15 2TT, United Kingdom

1161 ^eBritish Geological Survey, Environmental Science Centre, Nicker Hill,
1162 Keyworth, Nottingham NG12 5GG, United Kingdom

1163 ^fGeography and Environmental Science, Tower Building, University of
1164 Dundee, Dundee DD1 4HN, United Kingdom

1165 ***Corresponding author:** Leo Peskett, leo.peskett@ed.ac.uk

1166

1167 **Contents of this file**

1168 Number of pages: 9

1169 Number of figures: 5

1170 Number of tables: 4

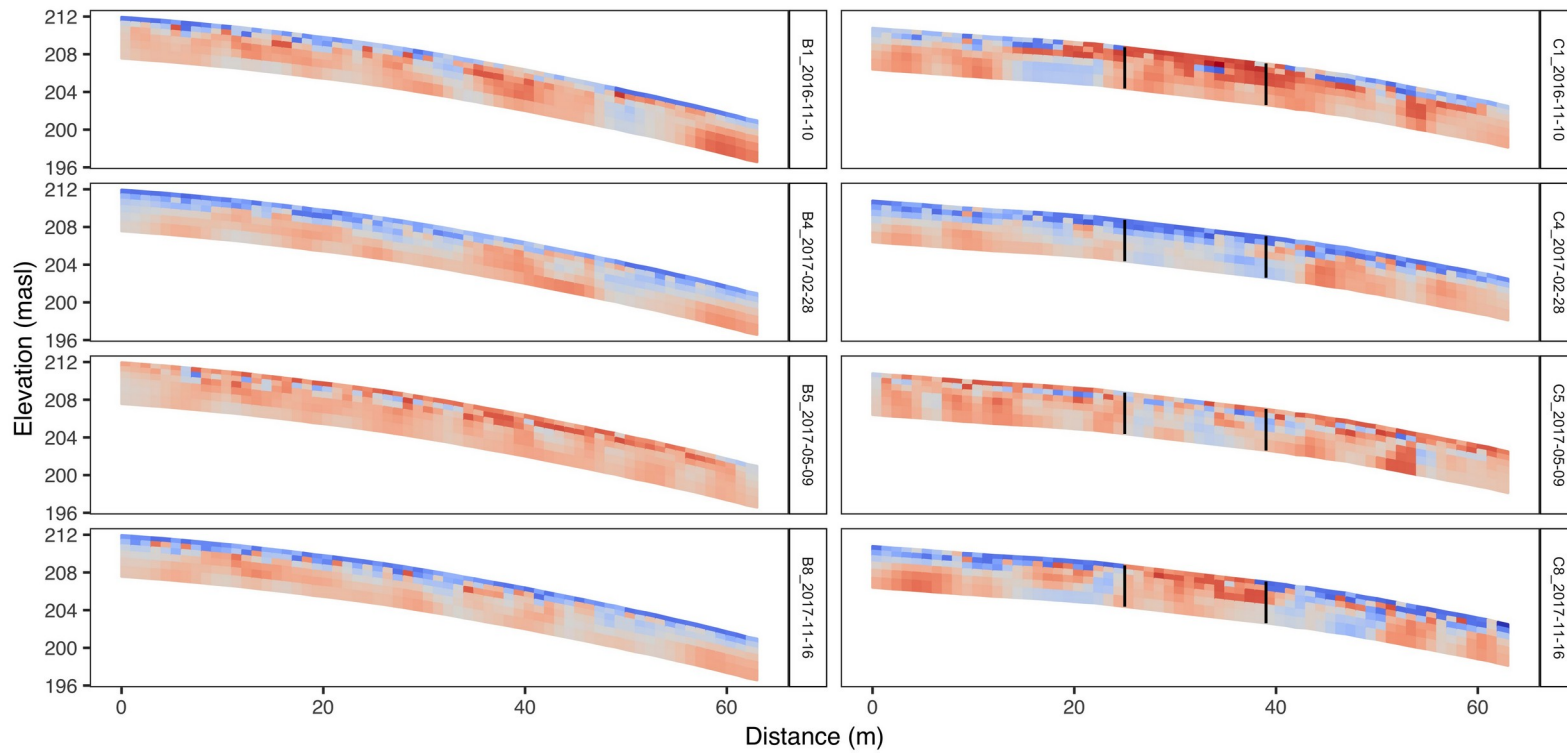
1171

1172

1173

1179 **Figure S2: Resistivity measurements in four surveys in different seasons relative to June 2017 survey.**

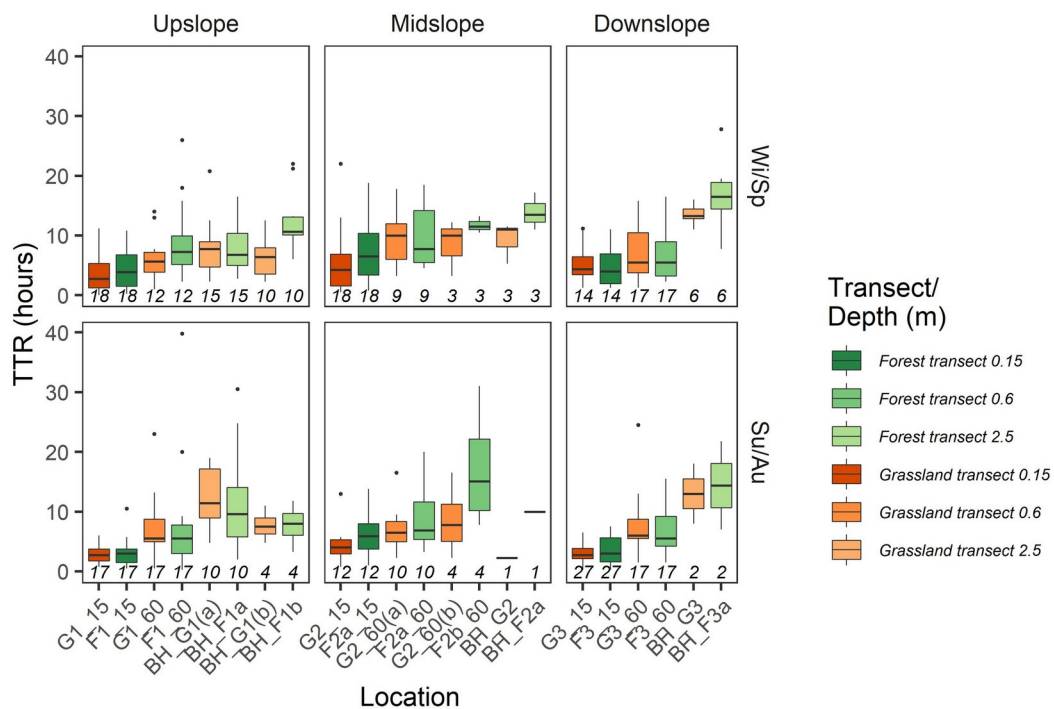
1180 **Black lines mark outside edges of forest strip.**



1181

1182

1183 **Figure S3: Pairwise comparison of soil moisture and groundwater**
 1184 **TTR between the two transects and between seasons for all**
 1185 **rainfall events analysed (n=52). Pairs are filtered to contain only**
 1186 **events when sensors on each transect responded and the event**
 1187 **sample size for each pair is denoted in italics. The horizontal line**
 1188 **inside the box represents the median and the lower and upper**
 1189 **hinges correspond to the first and third quartiles. The upper and**
 1190 **lower whiskers depict the largest and smallest values respectively**
 1191 **within 1.5 * the interquartile range (IQR). Numbers in italics show**
 1192 **the number of events in which sensor responded. Dots are**
 1193 **outliers.**



1194
 1195
 1196
 1197
 1198

1199

1200

1201 **Figure S4: a) Time to peak from the start of rainfall (TTPR) for the**
 1202 **different domains and depths on the forest strip and grassland**
 1203 **transects during nine rainfall events when the borehole**
 1204 **downslope of the forest responded and the majority of the other**
 1205 **soil moisture and groundwater sensors responded. b) Pairwise**
 1206 **comparison of soil moisture and groundwater TTPR between the**
 1207 **two transects and between seasons for all events (n=52). Pairs**
 1208 **are filtered to contain only events when sensors on each transect**
 1209 **are active and the event sample size for each pair is denoted in**
 1210 **italics. The horizontal line inside the box represents the median**
 1211 **and the lower and upper hinges correspond to the first and third**
 1212 **quartiles. The upper and lower whiskers depict the largest and**
 1213 **smallest values respectively within 1.5 * the interquartile range**
 1214 **(IQR). Numbers in italics show the number of events in which**
 1215 **sensor responded. Dots are outliers.**

1216

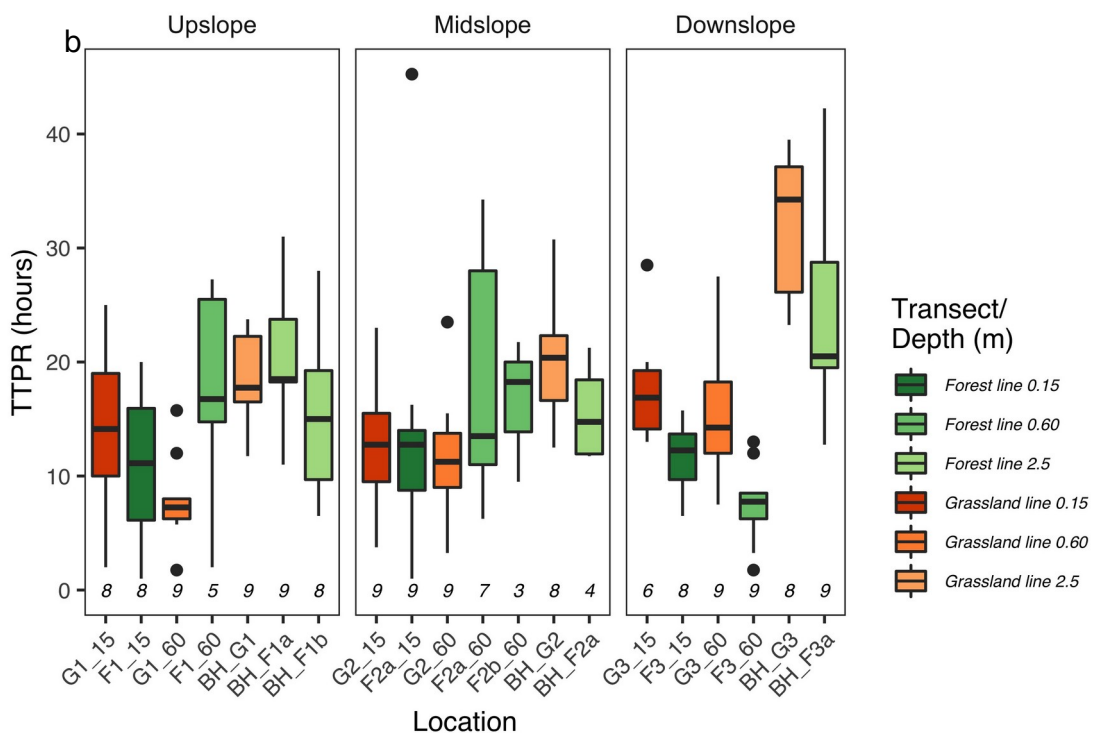
a
)

1217

1218

1219

1220



1221 **Table S1: Soil properties at each soil moisture sensor location**

<i>Location</i>	<i>Depth</i> (m)	<i>Clay</i>	<i>Silt</i>	<i>Sand</i>	<i>Gravel and cobbles</i> (% of total by mass)	<i>Organic content</i> (% of total by mass)	<i>Soil texture</i>
		(%fraction by volume)					
G1_15	0.15	9.83	65.4	24.8	37.0	6.95	Silty loam
F1_15	0.15	18.0	65.0	17.0	22.3	5.67	Silty loam
G1_60	0.60	12.1	48.6	39.3	55.5	2.03	Loam
F1_60	0.60	14.1	63.4	22.6	25.3	4.44	Silty loam
G2_15	0.15	15.3	63.6	21.1	53.4	4.91	Silty loam
F2a_15	0.15	10.7	53.7	35.6	49.0	1.97	Silty loam
F2b_15	0.15	11.2	64.8	24.0	26.1	5.73	Silty loam
G2_60	0.60	11.3	65.8	23.0	44.5	2.63	Silty loam
F2a_60	0.60	11.3	64.1	24.6	32.9	6.07	Silty loam
F2b_60	0.60	16.8	62.8	20.5	58.2	2.78	Silty loam
G3_15	0.15	11.5	60.0	28.6	44.6	5.19	Silty loam
F3_15	0.15	10.6	68.8	20.6	30.0	5.32	Silty loam
G3_60	0.60	13.5	67.7	18.8	40.7	4.20	Silty loam
F3_60	0.60	10.6	63.5	25.9	39.2	3.03	Silty loam

1222

1223

1224 **Table S2: Summary of rainfall events selected (n=52) and key**
 1225 **event characteristics used in the analysis. Percentage of sensors**
 1226 **responding is based on all working soil moisture and groundwater**
 1227 **sensors at the site (n=20).**

Rainfall start time	No. respondin g (%)	Total rainfall, TR (mm)	Intensity, I (mm h⁻¹)	AWI (mm)	AP28d (mm)
11/11/16 20:15	50	19.8	2.4	4.8	13.2
16/11/16 11:00	68	19.0	1.1	26.8	45.2
21/11/16 19:30	91	41.0	2.5	11.6	67.0
22/12/16 15:00	64	8.6	2.0	3.8	14.2
23/12/16 08:45	77	20.2	1.7	11.6	23.2
24/12/16 00:15	77	17.4	1.3	30.5	43.0
03/02/17 18:30	50	8.2	0.8	4.3	34.6
23/02/17 00:15	82	21.8	1.3	11.0	49.4
24/02/17 17:45	77	15.2	0.8	28.4	71.4
17/03/17 02:00	68	13.2	0.7	2.0	87.6
18/03/17 20:00	59	10.2	0.7	16.7	102
21/03/17 09:30	64	9.8	1.7	28.8	114
22/03/17 21:15	73	11.2	1.0	29.8	122
20/05/17 00:15	32	11.0	0.8	6.8	15.6
05/06/17 19:30	64	48.0	1.5	6.7	40.0
08/06/17 07:30	64	14.8	2.0	48.3	87.8
15/06/17 12:15	27	9.0	1.5	3.5	100
27/06/17 00:15	24	11.2	1.0	2.0	89.8
28/06/17 23:15	76	52.6	1.5	10.7	100
04/07/17 03:45	43	10.8	0.8	38.7	138
26/07/17 06:00	24	11.6	1.6	8.5	96.8
14/08/17 03:15	24	9.8	1.4	4.9	63.4
14/08/17 20:45	67	20.8	2.2	14.0	72.8
23/08/17 05:00	24	8.2	2.2	4.6	97.0
21/09/17 03:00	38	10.2	1.9	5.7	70.4
24/09/17 22:15	62	20.8	2.0	9.9	77.6
04/10/17 14:45	62	14.6	1.3	12.3	97.6
11/10/17 00:45	58	11.4	0.9	5.0	89.8
19/11/17 19:30	59	18.8	0.5	6.5	32.8
22/11/17 02:45	82	25.2	1.0	20.2	50.0
24/12/17 23:00	68	20.0	0.9	4.8	21.8
30/12/17 02:45	55	19.6	0.7	12.0	41.6
02/01/18 20:45	68	15.2	1.0	21.4	65.4
22/01/18 05:45	73	17.2	1.3	4.4	83.6
10/02/18 18:00	68	8.6	0.9	4.8	78.4
18/02/18 16:30	41	8.2	0.6	3.1	86.8
05/03/18 20:15	82	13.0	1.0	6.0	42.8
10/03/18 05:00	77	10.2	0.7	16.1	55.6
12/05/18 23:30	23	8.8	1.1	8.7	40.2
01/06/18 12:00	32	18.2	2.5	1.4	19.2
19/06/18 18:00	59	37.2	2.5	5.5	38.4
27/07/18 21:30	23	12.0	1.5	9.3	20.6
01/08/18 14:30	18	10.8	1.4	25.1	50.4
11/08/18 23:15	14	11.4	1.0	8.1	70.2
18/08/18 22:15	32	12.2	1.2	11.4	90.4
03/09/18 04:00	27	11.4	1.2	1.3	66.2
10/09/18 14:00	41	12.4	1.1	5.0	61.0
19/09/18 07:00	46	17.4	1.8	11.3	60.6
12/10/18 12:15	32	9.6	2.1	10.0	51.2
13/10/18 04:45	55	17.6	1.3	17.9	57.6
31/10/18 22:30	46	9.4	1.4	4.1	49.8
09/11/18 17:30	59	12.2	1.0	5.7	44.6

1228

1229

1230 **Table S3: Spearman rank correlation coefficients calculated to**
 1231 **compare relationships between different rainfall event**
 1232 **characteristics. * $p < 0.05$; * $p < 0.01$; *** $p < 0.001$.**

	<i>Rainfall (mm)</i>	<i>Intensity (mm h⁻¹)</i>	<i>AWI (mm)</i>
<i>Intensity (mm h⁻¹)</i>	0.32*	1.00	
<i>AWI (mm)</i>	0.00	-0.05	1.00
<i>AP28d (mm)</i>	-0.14	-0.08	0.33*

	<i>Time to response from the start of rainfall (TTR, h)</i>			<i>Time to peak from start of rainfall (TTPR, h)</i>			<i>Maximum absolute rise (MR, m³ m⁻³ for soil moisture and m for groundwater level)</i>		
	<i>All</i>	<i>Wi/Sp</i>	<i>Su/Au</i>	<i>All</i>	<i>Wi/Sp</i>	<i>Su/Au</i>	<i>All</i>	<i>Wi/Sp</i>	<i>Su/Au</i>
Soil moisture sensors									
Total rainfall (mm)	0.0286	-0.0043	0.136*	0.151***	0.232***	0.194**	0.295***	0.263***	0.271***
Intensity (mm h⁻¹)	-0.375***	-0.402***	-0.375***	-0.437***	-0.458***	-0.365***	0.225***	0.123	0.175**
AWI (mm)	0.0596	0.0152	0.0401	0.0121	-0.112	0.0771	0.0142	0.0768	-0.0376
AP28d (mm)	0.0306	0.081	0.0228	-0.000769	0.0627	0.0115	-0.132**	-0.225**	-0.0614
Piezometers									
Total rainfall (mm)	0.0844	0.146	-0.0714	0.121	0.152	0.0501	0.325***	0.287*	0.336*
Intensity (mm h⁻¹)	-0.262**	-0.337**	-0.396**	-0.309***	-0.294*	-0.434**	0.181*	0.241*	0.0416
AWI (mm)	0.0118	-0.0138	0.0465	-0.232*	-0.39***	-0.0314	-0.113	-0.169	0.0764
AP28d (mm)	0.00493	-0.0214	0.0614	-0.0755	-0.0677	-0.0686	0.00722	-0.141	0.250

1233 **Table S4: Spearman rank correlation coefficients between rainfall event characteristics / antecedent conditions**
1234 **and response metrics for all soil moisture sensors and for all piezometers across both the forest strip and**
1235 **grassland transects. Coefficients are shown for all events (n=52) and separately for events in Winter/Spring**
1236 **(Wi/Sp, n=20) and Summer/Autumn (Su/Au, n=32). * $p < 0.05$; ** $p < 0.01$; *** $p < 0.001$.**

